Saskatchewan Agriculture, Food and Rural Revitalization

ADF

AGRICULTURE DEVELOPMENT FUND

FINAL REPORT

19990309

DEVELOPMENT OF DRYING EQUIPMENT FOR HEAT SENSITIVE MATERIAL

Funded by:
The Agriculture Development Fund

Juiy 2003

Prepared by: University of Saskatchewan

104-00731/

FINAL PROJECT REPORT
JUNE 2003

TITLE: An Investigation of Heat Pump Systems for Low Temperature Drying of Specialty Crops

SUBMITTED TO: Saskatchewan Agriculture and Food, Canada

SUBMITTED BY: Drs. G.J. Schoenau and S. Sokhansanj

College of Engineering, University of Saskatchewan,
57 Campus Drive, Saskatoon, Canada - SK S7N 5A9

Contact Person: Dr. Greg J. Schoenau
Phone: (306) 966 – 5446
Fax: (306) 966 – 5427
Email: Greg_J_Schoenau@engr.usask.ca

Abstract

High value specialty crops such as ginseng, herbs and echinacea need to be dried at low temperatures for product quality optimization. This is an important consideration as they have a relatively high commercial value. Heat pump dryers operating under closed loop conditions have the potential to dry these crops, independent of ambient conditions and at low temperatures (30-45°C). To study their performance, two types of prototype heat pump dryer systems were designed, constructed and field-tested. The first system was a small fixed bed cabinet dryer and the other dryer was a full scale prototype moving bed cross flow system. The cabinet dryer was considered suitable for small growers of specialty crops, while the continuous bed dryer could be used for large scale commercial drying of heat sensitive agricultural products. The heat pump dryer systems were evaluated using several specialty crops (alfalfa, catnip, wormwood, red clover, portulaca, dandelion and ginseng). Specialty crops with chopped aerial components utilized continuous bed drying, while whole aerial plant and root crops were dried using static bed or batch process. The heat pump drying system was found to be both faster and more energy efficient than conventional drying methods. It took 5 days and 190 kWh of energy to reduce the average moisture content of ginseng roots below 10%, while commercial dryers currently in use would take on an average 14 days and 244 kWh of energy. The re-circulating nature of the heat pump dryer makes it 22% more energy efficient and reduces the drying time by 65%, compared to conventional dryers. Finally, a heat pump dryer simulation model was developed using the fundamentals of heat and mass transfer, and was validated against the experimental results. A computer program was developed based on the validated model. This program can be modified and used to size a heat pump dryer system for a given product and material through put.

Executive Summary

Timely drying of the fresh material is essential in producing high quality products, preventing spoilage and prolonging the shelf life of active ingredients in the products. Discoloration, shrinkage and degradation of active ingredients limits the upper temperatures that can be used in the drying of heat sensitive material. The primary objective of this project is to develop a low temperature (near ambient air temperatures) dryer suitable for drying specialty crops (such as ginseng, catnip, wormwood, echinacea, etc.). Low temperature drying is generally considered very important in preserving the quality of these commercially valuable crops. A re-circulating type heat pump dryer was selected as the best means of achieving this low temperature drying as low temperature air can be de-humidified to raise its drying potential.

The project was divided into three main tasks; the construction of a prototype dryer, testing the dryer performance and providing a computer based simulation model for predicting dryer performance. This report details the procedures followed and results obtained to accomplish each of these tasks.

TASK A

Design and Construction of Prototype Heat Pump Dryer Systems

Two types of prototype heat pump dryer systems were designed, constructed and field-tested during the years 2000-02. These systems were distinguished from each other based on the techniques followed to dry specialty crops. The first system was a fixed bed cabinet dryer and the other dryer was a moving bed cross flow system. The motivation for constructing two different dryers was based on their relative size and cost. The small cabinet dryer used stacked wooden mesh trays and two relatively inexpensive household de-humidifiers to accomplish drying, while the continuous bed prototype dryer utilized conveyor belts and a custom-built commercial heat pump system. The continuous bed heat pump dryer was relatively expensive, however, it was able to dry large quantities of material. The cabinet

dryer was considered suitable for individual use by small growers of specialty crops, while the continuous bed dryer could be used for commercial production of heat sensitive agricultural products. This system could be useful for a very large scale grower or in a co-operative or central organization that would serve several small growers.

TASK B

Experimental Evaluation of Heat Pump Dryer Performance

Experiments were performed using both the cabinet and continuous bed heat pump dryers. Chopped alfalfa was used to evaluate the performance of the cabinet dryer. The reason for using alfalfa instead of specialty crops was that its drying properties were known and the material was readily available. Also the structure of alfalfa leaves and stems is similar to that of many herbs and specialty crops, which helped in validating the simulation model of the heat pump dryer system (Task C).

Chopped alfalfa, initially at 70% moisture content, was dried to 10% moisture content in the cabinet dryer. Two dryer setups were used. The dryers in each case had a partitioned cabinet with trays of material on one side and a stack of one or two small household dehumidifiers on the other side. Air was re-circulated through the material from bottom to the top and back through the dehumidifiers. Two drying configurations were tested. In one, the material was left on the trays until drying was complete (batch or fixed tray drying). In the other configuration, the trays were moved from top to bottom, introducing a new tray at the top while removing an old tray from bottom. Drying air temperature ranged from 25°C to 45°C. Alfalfa chops dried in 5 h in the fixed tray and in 4 h in the moving tray drying. The dehumidifiers used in this study were about 50% more efficient in recovering the latent heat from the dryer exhaust air than conventional dryers. Moving tray drying was faster than stationary tray drying by about 11% and more energy efficient. Moving tray drying is potentially a better option than fixed tray drying because it results in high humidity ratios at the entrance of evaporator and, constant specific moisture extraction rates can be maintained.

The prototype continuous bed heat pump drying system was evaluated using several specialty crops. The range of specialty crops was limited by availability. Static bed (stationary conveyor belts) as well as continuous bed (moving conveyor belts) drying experiments were performed using the prototype heat pump dryer system. The choice of experiments conducted (static or continuous) was determined based on the type of material dried. Specialty crops were divided into two categories based on the part of the plant used. The first category had crops with leaf and stem material (aerial parts) while the other category had roots.

Specialty crops with chopped leaf and stem material (alfalfa, catnip, wormwood and red clover), and sliced carrots utilized continuous drying, while whole aerial (alfalfa and red clover), portulaca (purslane) and root crops (carrot, dandelion and ginseng) were dried using static bed or batch process. With the exception of carrots, all of these crops (including alfalfa) are being marketed or are under development (portulaca and dandelion roots) as herbal type medicines. Carrots were selected to provide preliminary and comparative data for roots such as ginseng, which were expensive and only available in limited quantities. The experiments determined that the drying rate of chopped alfalfa, wormwood and red clover was similar. Catnip had a slightly higher drying rate, which could be due to comparatively bigger pores on its leaves and stems which helped moisture to escape more readily compared to the other material. Chopped portulaca dried almost three times slower than other chopped aerial crops. This was due to high moisture content and sticky nature of chopped aerial parts of portulaca, which caked while drying and did not allow hot and dry air to pass through, exposing less surface area for drying. It was also observed from drying results that chopped aerial crops dried almost seven times faster than whole aerial parts (alfalfa and red clover). This could be due to lower surface area to mass ratio of the whole aerial crops. On the other hand, the drying rate of whole roots (carrot, dandelion and ginseng) took substantially longer than the aerials. The average initial moisture content of roots was about 69% with carrot as the exception at 88% moisture content. The whole roots were dried at an average temperature of 35°C. It was found that the drying time for all the three root types was different. The difference was primarily due to their initial moisture content and physical structure. Dandelion had the fastest drying time as it took only 53

hours to dry. Carrots had the next highest drying time of 81 hours and finally ginseng, which took about 120 hours to dry. It was observed that ginseng root was composed of two layers. The outer layer dried quickly and shrunk to form a hard and thick layer. This layer significantly reduced moisture diffusion from inside of the root to ambient air.

The heat pump drying system was both faster and more efficient than conventional drying methods. The prototype continuous bed dryer took 5 days and 190 kWh of energy to reduce the average moisture content of ginseng roots below 10%, while commercial dryers currently in use were reported to take on an average 14 days and 244 kWh of energy. The re-circulating nature of the heat pump dryer makes it 22% more energy efficient and reduces the drying time by 65% compared to conventional dryers.

The results also showed that energy consumption during drying increased almost by three folds with the decrease in surface area to mass ratio of whole aerial crops compared to chopped material. Therefore, it is advised to chop the aerial crops in order to expedite the drying process.

The drying results of catnip, wormwood, red clover, portulaca, whole and sliced roots of carrots and dandelion were not compared, as no relevant published experimental data could be found.

TASK C

Development and Validation of a Computer Based Dryer Model

A heat pump dryer simulation model was obtained by merging a heat pump and a dryer model. These models were prepared separately and later unified using the laws of heat and mass transfer. It was decided to first perform a few preliminary experiments using the small cabinet dryer to validate the model (Task B). In a continuous drying system, psychrometric properties do not change significantly over time. Hence, the verification of a computer model is difficult, as there will be only a single set of data from each experiment. Using tray or batch drying, at least ten sets of data can be generated from each experiment. In

stationary tray drying, the psychrometric properties of air are transient and the data sets obtained are useful in establishing the accuracy of the simulation model. The small and less expensive cabinet dryer also provides an alternate heat pump drying system that could be adopted by small growers.

Experimental data sets obtained from the cabinet dryer were compared with the simulation results of heat pump model. An error and/or difference between the predicted and measured temperatures of ±4°C at the condenser coil and ±5°C at the evaporator coil were observed. All the curves generally showed good agreement in the temperature variation pattern.

A simulation model for the prototype continuous bed heat pump dryer was developed to predict its performance. The dryer performance includes finding drying rate of the material and psychrometric conditions of the air, and also to determine the refrigerant mass flow rate and corresponding temperatures at the condenser and evaporator coils of the heat pump system. The accuracy of the predicted results was verified from our experiments.

The preliminary results from the prototype continuous bed heat pump dryer simulation indicated that the different dryer air inlet temperatures (30°C, 40°C and 50°C) has an insignificant effect on the drying rate of alfalfa. Therefore, based on the results, it was concluded that the dryer inlet air temperatures could be kept as low as 30°C, if required, to maintain product quality and save energy. Drying experiments were performed based on the preliminary predictions. Alfalfa was dried at a temperature of 30°C with an initial moisture content of 67%, material flow rate of 2.9 kg/h and a material bed thickness of 0.03 m. The final moisture content of alfalfa after 3.3 h of drying was 10.4%. Using the simulation model for the prototype heat pump dryer, the results for alfalfa drying were predicted. At similar drying conditions (same as used in the experiment), the final moisture content of alfalfa was predicted to be 9.4%. Which is very close to the measured value.

The experimental humidity ratio of air at dryer exit was determined, when the material mass flow rate was in the range of 2.0 – 4.5 kg/h. It was found from psychrometric chart that the average value of humidity ratio was about 5.5 g/kg of dry air. This value also agrees with

the predicted air humidity ratio. The mass flow rate of alfalfa was in the range of 2.0 – 4.5 kg/h, indicating that it might be advisable to use the prototype heat pump dryer in combination with some other drying technique, which can enhance its drying rate. It was also felt that the conveyor-belt system was too small and that a larger system, exposing more material could increase the dryer through put.

A similar computer based simulation model was also developed to determine proper size of a drying chamber, airflow rate and psychrometric properties of air to help in the appropriate selection of a heat pump.

A user's manual and programmer guide for both heat pump dryer and drying chamber design simulation models are provided in Appendix C. The simulation model can be used for parametric design of heat pump dryer systems.

TECHNICAL REPORT

Table of Contents

Page

TITLE.....1
ABSTRACT.....2
EXECUTIVE SUMMARY.....3
LIST OF FIGURES.....12
LIST OF TABLES.....14
NOMENCLATURE.....15
1. BACKGROUND.....20
2. PROJECT OBJECTIVES.....24
3. TASK A - Design and Construction of Prototype Heat Pump Dryer Systems.....25
3.1 Re-circulating Cabinet Dryer.....25
3.2 Moving Bed Prototype Heat Pump Dryer.....28
4. TASK B - Experimental Evaluation of the Cabinet and Continuous Bed Dryers.....31
4.1 Instrumentation of Prototype Heat Pump Dryer.....31
4.1.1 Instrumentation.....31
4.1.2 Experimental Procedure.....32
4.1.3 Results and Discussion.....33
4.1.3.1 Energy and Mass Balance.....41
4.1.3.2 Measured Psychrometric Conditions of Process Air.....43
4.2 Experimental Evaluation of Prototype Heat Pump Dryer.....45
4.2.1 Instrumentation.....45
4.2.2 Determination of Material Moisture Content.....46
4.2.3 Preliminary Experimental Results.....47
4.2.4 Experimental Results for Several Crop Materials.....48
4.2.5 Energy Calculations.....54
5. TASK C – Computer Based Heat Pump Dryer Model.....57
5.1 Dryer Model – Thin Layer.....57
5.1.1 Drying Rate Equation.....58
5.1.2 Mass Balance Equation.....60

5.1.3 Energy Balance Equation.....60
5.1.4 Heat Transfer Equation.....61
5.2 Heat Pump Model.....62
5.2.1 Overall Heat Transfer Coefficient at Condenser Coil.....64
5.2.2 Overall heat Transfer Coefficient at Evaporator Coil.....65
5.2.3 Compressor and Expansion Valve Model.....67
5.3 Model Validation.....68
5.3.1 Validation of Simulation Model Using Cabinet Dryer Results.....69
5.3.2 Validation of Continuous Bed Prototype Heat Pump Simulation Model...71
6. CONCLUSIONS.....74
REFERENCES.....76
APPENDIX A: Equations used for Modeling Refrigerant used in Cabinet Dryer.....79
A.1 Condenser and Evaporator Coil Specifications.....79
A.2 Thermophysical Properties of R 134A.....80
A.3 Fin Efficiency.....83
APPENDIX B: Equations used for Modeling Refrigerant used in Prototype Heat Pump Dryer 86
B.1 Condenser and Evaporator Coil Specifications.....86
B.2 Thermophysical Properties of R 404A.....87
APPENDIX C: Computer Simulation Model, Users Guide.....92
C.1 Combined Heat Pump Dryer System.....92
C.2 Heat Pump Dryer Sizing.....97
INDICATION FOR FURTHER DEVELOPMENT.....101
LIST OF JOURNAL PUBLICATIONS AND CONFERENCE PRESENTATIONS.....102
PERSONNEL.....103
INFORMATION OF BENEFITS TO PRODUCERS, PROCESSORS OR GOVERNMENT 104
STATEMENT OF RECEIPTS AND EXPENDITURES.....105

List of Figures

Title Page

1. Block diagram of the experimental dehumidifier system showing one dehumidifier....26
2. Block diagram of the experimental dehumidifier system showing two dehumidifiers....27
3. Overview of prototype cross-flow continuous bed heat pump dryer system....28
4. Schematic sectioned view of the counter cross-flow continuous bed drying chamber....29
5. Schematic block diagram of the commercial heat pump system....30
6. Typical measured temperature and relative humidity of air at the dryer entrance and exit for experimental number 12....37
7. Typical measured moisture condensation during fixed and moving tray drying with time for experiment number 12....38
8. Specific moisture extraction rate and instantaneous power consumed by heat pumps over the drying process for experiment number 12....39
9. Typical moisture content of material in individual trays over drying time for experiment number 12....41
10. Measured psychrometric condition of process air with air bypass around evaporator coils and non-adiabatic drying....44
11. Block diagram o prototype heat pump dryer system depicting the locations of instrumentation....45
12. Change in moisture content of different roots over drying time....52
13. Fresh dandelion roots....53
14. Dried dandelion roots....53
15. Fresh carrots....53
16. Dried carrots....53
17. Dried carrots (sliced)....53
18. Fresh ginseng roots....54
19. Dried ginseng roots....54
20. Psychrometric and material conditions at the two elemental volumes on conveyors one and two....58

21. Actual heat pump cycle.....63
22. Ideal heat pump cycle.....63
23. Modeled pressure-enthalpy diagram for refrigerant cycle.....67
24. Basic schematic diagram of the cabinet heat pump dryer system.....69
25. Comparison of measured and simulation temperatures of refrigerant at condenser and evaporator coils (during batch drying).....70
26. Moisture extraction rate for experimental and simulation results over material drying time (batch process only).....71
27. Predicted affect of alfalfa mass flow rate on its moisture content at the dryer exit.....73
28. Pressure-enthalpy diagram for a refrigerant.....80
29. Pressure-enthalpy diagram for a refrigerant.....88

List of Tables

Title	Page
1. Heat pump dehumidifier specifications	27
2. Instrumentation used in the tests for the second setup	32
3. Summary of data from experimental drying of alfalfa chops in a re-circulating air cabinet using household dehumidifier	35
4. Calculations for energy balance	42
5. Calculations for mass balance	43
6. Instrumentation used in the tests on the prototype heat pump dryer	46
7. Material moisture content	47
8. Results of preliminary alfalfa drying experiments	48
9. Drying characteristics for several leaf and stem material (aerial) and root crops	50
10. Calculations for energy balance of the prototype heat pump dryer	55

Nomenclature

A_c	total surface area of condenser coil, m^2
A_{dsh}	area of desuperheating section of condenser coil, m^2
A_f	total condenser fin area, m^2
A_F	total evaporator fin area, m^2
A_{oc}	surface area of the condenser coil, m^2
A_{oe}	surface area of the evaporator coil, m^2
A_{pie}	inside evaporator pipe area, m^2
A_{po}	outside pipe evaporator area, m^2
A_{ti}	inside condenser tube area, m^2
A_{to}	outside condenser tube area, m^2
AMTD	arithmetic mean temperature difference
ASHRAE	American Society of Heating Refrigerating and Air-conditioning Engineers
b_{wm}	coefficient evaluated at water film temperature, kJ/kg-°C
C	capacity rate ratio, C_{min}/C_{max}
C_{min}	smaller capacity rate ($m_r C_{pr}$ or $m_a C_{pa}$ whichever is smaller), kJ/sK
COP_{HP}	Coefficient of performance of heat pump (dimensionless)
COP_{ref}	Coefficient of performance of refrigerator (dimensionless)
C_p	specific heat, J/kgK
C_{pa}	specific heat of air, kJ/kgK
C_{pg}	specific heat of material, kJ/kgK
C_{pl}	specific heat of liquid, kJ/kgK
C_{pw}	specific heat of water vapor, kJ/kgK
C_{rdsh}	capacity rate for refrigerant, $m_r C_{pr}$, kJ/sK
D_{eqv}	equivalent fin diameter, m
D_i	inside coil diameter, m
D_o	coil outside diameter, m

E	enhancement factor
G	mass velocity, kg/m^2s
G_a	mass flow rate of air, kg/m^2s
G_p	mass flow rate of material, kg/m^2s
H	moist air enthalpy calculated at average air temperature, J/kg
H	enthalpy of saturated air, kJ/kg
h_a	convective heat transfer coefficient, W/m^2K
h_{cow}	convective heat transfer coefficient for outside surface, kW/m^2K
h_{cv}	heat transfer coefficient, kJ/m^3minK
h_f	forced convective heat transfer coefficient, W/m^2-K
h_i	inside (refrigerant) heat transfer coefficient, W/m^2-K
h_{NcB}	nucleate pool boiling coefficient, W/m^2-K
h_o	outside (air) heat transfer coefficient, W/m^2-K
h_{ow}	outside wet convective heat transfer coefficient, W/m^2-K
H_{sR}	moist air enthalpy calculated at average refrigerant temperature, J/kg
H_{st}	the assumed enthalpy of saturated moist air evaluated at tube temperature, kJ/kg
i_{fg}	latent heat of vaporization, J/kg
k	drying rate constant, min^{-1}/ h^{-1}
k	thermal conductivity of air, W/mK
k_f	thermal conductivity of fin, W/mK
k_w	thermal conductivity of water, W/mK
L	total length of coil, m
L_g	latent heat of vaporization of moisture from material, kJ/kg
LMTD	logarithmic mean temperature difference, ^oC
MR	moisture ratio (fraction)
M	moisture content at time t
M	molecular weight
M_e	equilibrium moisture content
M_o	initial moisture content

MER	moisture extraction rate, kg/h
$\dot{m}_a$	mass flow rate of air, kg/s
$\dot{m}_r$	mass flow rate of refrigerant, kg/s
N_r	number of rows
Nu_{anr}	Nusselt number for N_r rows at AMTD
Nu_{a3r}	Nuselt number for 3 rows at AMTD
NTU	number of transfer units
P	atmospheric pressure, Pa
P_{crit}	critical pressure, Pa
P_l	longitudinal distance between rows, m
Pr	Prandtl number for air
P_{rp}	reduced pressure = P/P_{crit}
Pw	vapor pressure, Pa
P_{ws}	saturated vapor pressure, Pa
q_1	energy supplied to maintain body B at higher temperature T_1, J
q_2	energy extracted from the surroundings at temperature T_2, J
RH	relative humidity, %
S	suppression factor
SMER	specific moisture extraction rate, kg/kWh
t	time, min
T	temperature, K
T_a	temperature of air, °C
t_{aci}	temperature of air before entering the condenser coil, °C
T_{ao}	initial temperature of air, °C
t_{as}	temperature of saturated air, °C
T_g	temperature of agricultural material, °C
T_{go}	initial temperature of agricultural material, °C
t_R	refrigerant temperature at saturation, °C
t_{rci}	temperature of refrigerant at condenser inlet (or at compressor outlet), °C

t_{rs}	temperature of refrigerant at vapor saturation curve, °C
t_t	total time, min
t_t	tube temperature, °C
TPC	first predicted value of refrigerant temperature at the condenser, °C
TPE	first predicted value of refrigerant temperature at the evaporator, °C
$\Delta T_{LMTDCond}$	log mean temperature difference taken at the condenser coil, °C
T_1 & T_4	temperature of process air at the condenser outlet and inlet (refer to Figures 2.3 and 2.4), °C
U_{dsh}	overall heat transfer coefficient for desuperheating section of condenser, W/m^2K
U_{oe}	overall heat transfer coefficient at the evaporator coil, $kg/m^2/s$
U_{oc}	overall heat transfer coefficient at the condenser coil, $W/m^2/K$
v	velocity of refrigerant, m/s
V_{fin}	air velocity between fins for a tubeless heat exchanger, m/s
W	humidity ratio, kg/kg dry air
W_e	work input to the heat pump (compressor), W
W_f	fin spacing, m
W_o	initial humidity ratio, kg/kg
W_1	humidity ratio of air before entering the evaporator, kg/kg dry air
W_2	humidity ratio of air after passing through the evaporator, kg/kg dry air
x	thickness of the dryer bed, m
X	liquid mass fraction
X_L	longitudinal distance between coil rows, m
X_T	transverse distance between coil rows, m
y	material movement direction along the dryer bed
Y_f	fin thickness, m
y_w	thickness of water film, m
z	direction along the width of dryer bed
Z_{eqv}	equivalent fin height, m
β	ratio of tubeless crossectional area to fin surface area including tube area

ε	effectiveness
μ	viscosity, Ns/m^2
μ_a	air viscosity, Ns/m^2
ρ	density of refrigerant, kg/m^3
ρ_a	air density, kg/m^3
ϕ	surface heat flux, W/m^2
ϕ_{eff}	fin efficiency

1. Background

Specialty crops such as ginseng, herbs, echinacea, etc., need to be dried at low temperatures (30-45°C) for product quality optimization. This is an important consideration as they have a relatively high commercial value. Heating ambient air to use for drying, although a simple cost-effective procedure, is of limited application, particularly at higher ambient air relative humidities because of the low allowable maximum temperature conditions. High temperature drying deteriorates the material structure and can render it unsuitable for further use. Heat pump dryers operating under closed loop conditions have the potential to dry these crops, independent of ambient conditions. Under high ambient moist air conditions, it may not even be possible to dry the material by conventional means.

Heat pump dryers (HPD) have the potential to operate more efficiently, and at lower temperatures than conventional dryers (Filho and Strommen, 1996). In fact for low temperature (30°C to 45°C), conventional heated air drying may not be able to be used at all if the outdoor temperature and relative humidity are higher. In HPD, both sensible and latent heat can be recovered from the dryer exhaust air, improving the overall thermal performance. Latent heat is recovered by dehumidification of air at the evaporator. Dehumidification is achieved by cooling the vapor-air mixture below the dew point temperature. The heat pump drying system is a combination of two sub-systems: a heat pump and a dryer.

Hodgett (1976) and Tai et al. (1982) studied the advantages of the heat pump dryers compared with conventional dryers. According to Hodgett the specific moisture extraction rate (SMER) for heat pump drying is in the range of 1.0 – 4.0 kg/kWh, whereas the SMER for a conventional dryer is in the range of 0.2 – 0.6 kg/kWh. Tai et al. (1982) studied five different batch drying/dehumidification systems, including three with heat pumps and compared them on the basis of specific power consumption and primary energy consumption. They observed that the efficiency of each system improved as the relative humidity of the air leaving the dryer increased. The systems were most efficient when run at a minimum relative humidity of 30%. A closed cycle heat pump dryer proved to be the

most advantageous of the five systems. These studies were based on simple models, which did not take account of the detailed heat and mass transfer phenomena taking place at the evaporator and condenser coils.

Oliver (1982) conducted research on the drying of wool, clay and timber with a dehumidifying heat pump. He suggested that the heat pump based dryer was more efficient when the drying temperatures required are no more than 50°C with an average relative humidity during drying at the dryer exit of well above 30%. This statement agrees with the results obtained by Tai et al. (1982) and Baines (1986). According to Baines (1986), the maximum temperature limit varies depending on the refrigerant and equipment used. Baines (1986) concluded from his studies that using heat pumps in dryers reduces the energy loss incurred by the heating and evaporation processes that are energy inefficient in the simple heat and vent dryer. He obtained SMER in the range of 1.0 – 6.0 kg/kWh compared to that of 1.0 – 4.0 kg/kWh obtained by Hodgett (1976). According to Strommen and Kramer (1994), heat pump dryers produces a higher quality product compared to traditional oil fired dryers. Filho and Strommen (1996) used a pilot scale heat pump dehumidifier for drying biomaterial, which demonstrated a reduced energy consumption of up to 60-80%. Prasertsan and Saen-saby (1998) dried sawed wood and bananas using a heat pump dryer. The maximum SMER was 0.572 kg/kWh to dry sawed wood to less than 10% moisture content.

Heat pump dryers have been studied for both batch and continuous dryers. Although heat pump-assisted batch dryers have proven to be economical compared to conventional heated air dryers, their acceptance by the agricultural industry has been slow. The reason is the difficulty in controlling the process to achieve a high efficiency. In batch drying the moisture content of material decreases with time and hence the relative humidity (RH) of the air inside the drying chamber. After a certain time period, the RH usually goes below 25 to 30%. The amount of power consumed remains the same even though the moisture condensed at the evaporator decreases. Tai et al. (1982) showed that the power consumption per kilogram of moisture removed (the reverse of SMER) in a heat pump assisted dryer was a minimum when the RH of the drying chamber was maintained above 30%.

Sosle et al. (2000) batch dried apple slices from 70% to 13% moisture content at 30°C using a heat pump. They found that the final quality of the product in terms of consumer preference was excellent. The chewability and mouthfeel of the product were much appreciated in the case of the low temperature processed product. Microscopic examination of freehand sections showed that the cell wall structure remained in an extremely good shape and the cells regain their shape and size to a remarkably good extent upon re-hydration.

Achariyaviriya et al. (2000) batch dried papaya glace at 50°C using a heat pump. The specific airflow rate of 40.2 kg/h-kg dry product was used. The fraction of evaporator bypass air was 0.63 and the initial and final moisture contents were 40.4% and 23.2% (db), respectively. MER and SMER values obtained from the experiment were 0.171 kg-water/h and 0.091 kg-water/kWh, respectively.

Continuous dryers, where the material is fed and discharged at a uniform rate, are also configured with heat pumps. Unlike batch dryers, the continuous dryers are much easier to control since the energy flows and temperatures are constant, as the material is uniform and flows through at a constant rate. Very few studies have been done on heat pump assisted continuous dryers compared to heat pump assisted batch dryers. The most significant work was done by Clements et al. (1993). They used wetted foam rubber as the test material in a continuous heat pump dryer. The initial moisture content of the foam was 64% (wb). They showed that when the RH of the air at the dryer exit was increased from 32% to 80%, the SMER of the dryer doubled from 1.25 to 2.5 kg/kWh. To maintain a minimum relative humidity of 30% inside the dryer, the foam feed rate was kept at 11.5 kg/h. The relative humidity of air entering the evaporator increased to 80% when the product feed rate was increased to 28.5 kg/h. In spite of the increased SMER, they did not dry the material to below 18% moisture content, which is quite high for safe storage of most agricultural crops. Another drawback of their study was that they performed drying tests on foam rubber instead of on hygroscopic agricultural materials. Because there have been few studies, more detailed study is required to understand and explore the operating characteristics of heat pump assisted continuous dryers using crop material.

Many models have been developed to describe heat and mass transfer taking place in the HPD system. Those systems were either too complicated to be applied for different dryer configurations or were not accurate enough to calculate the heat and mass transfer at the condenser and evaporator coils. There is a need to design a HPD, which can be used by growers for drying specialty crops. A simplified mathematical model of a heat pump assisted crop dryer was developed which can be applied to different configurations. Experimental tests verified that the model can also predict crop drying rates with sufficient accuracy to be used for this purpose.

2. Project Objectives

This project is concerned with the technology of heat pump assisted drying of specialty crops, the benefits and potential of the process in agriculture sector. The purpose of using heat pump for drying of specialty crops is to dry them at a lower temperature than would otherwise be possible using conventional drying techniques. Low temperature drying of specialty crops reduces the risk of loss in nutrient content and damage to physical properties which are important aspects considering their high commercial value. Heat pump drying is also potentially more energy efficient since it is possible to recover latent heat from the humid dryer exhaust air. The present project has been divided into three stages (or Tasks).

TASK A The design and construction of Cabinet and Continuous Bed prototype dryer systems.

TASK B Field-testing of prototype heat pump dryers using specialty crops or crops with similar characteristics.

TASK C To develop a comprehensive computer model using the fundamentals of thermodynamics for a heat pump dryer system.

3. TASK A – Design and Construction of Prototype Heat Pump Dryer Systems

Two types of prototype heat pump dryer systems were constructed and field-tested during the years 2000-02. These systems were distinguished from each other based on the techniques followed to dry specialty crops. The first system was a small fixed bed cabinet dryer and the other, much larger system, was a moving bed cross flow dryer. These systems were designed primarily based on the information developed during the M.Sc. thesis work of Adapa (2001).

3.1 Re-circulating Cabinet Dryer

Two dryer setups were considered. In the first setup, a cabinet dryer consisting of a chamber and a dehumidifier were assembled (Figure 1). The chamber was partitioned into left and right side compartments with air circulating through the compartments in a clockwise direction. Five trays were stacked in the left compartment to support the drying material. A household type dehumidifier was placed in the right compartment for air conditioning. The dehumidifier had a condenser and an evaporator coil, which provided the heating and cooling/dehumidification for the process air in the dryer. A fan was built into the dehumidifier, which was used to drive the air through the coils. The fan also provided airflow for the re-circulating loop. The walls of the chamber were insulated with 51 mm thick fiberglass insulation. The doors of the cabinet were sealed to avoid air leaks using foam rubber strips.

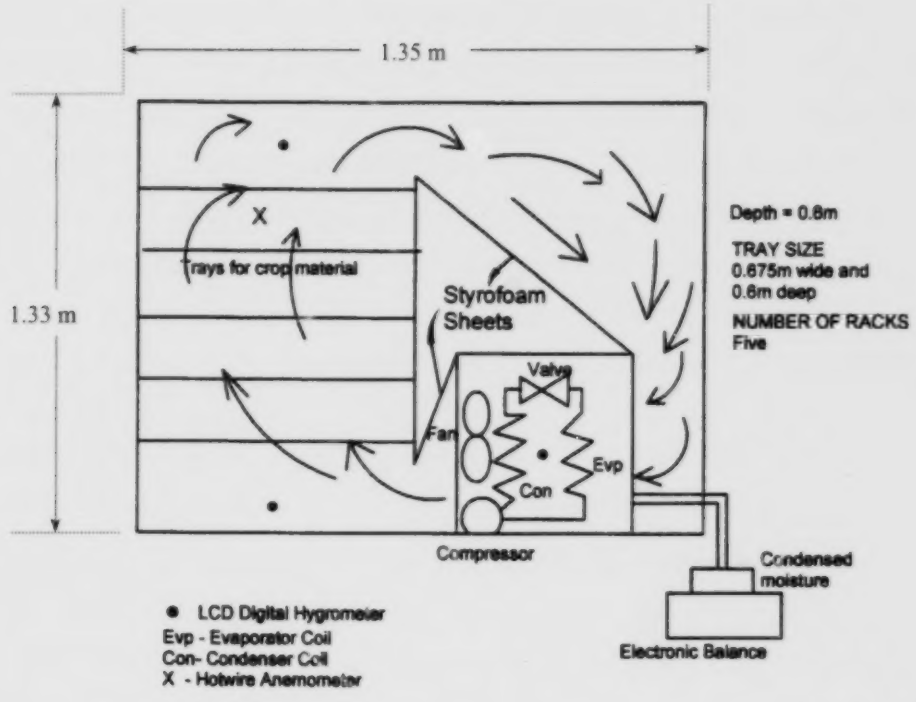

Figure 1. Block diagram of the experimental dehumidifier system showing one dehumidifier

Six preliminary experiments were performed using the arrangement of equipment shown in Figure 1. The results obtained and the operating conditions of this dryer led to a modified and improved dryer setup (Figure 2). This new setup also had left and right side compartments, similar to the first setup. Nine trays were stacked in the left compartment, while two dehumidifiers of the same capacity were stacked in the right compartment. An improved layout of instrumentation was done to record appropriate parameters (instrumentation will be discussed in section 4.1.1). The household dehumidifier specifications are given in Table 1. The material and equipment costs for this cabinet dryer was about $1000. Construction costs are not included.

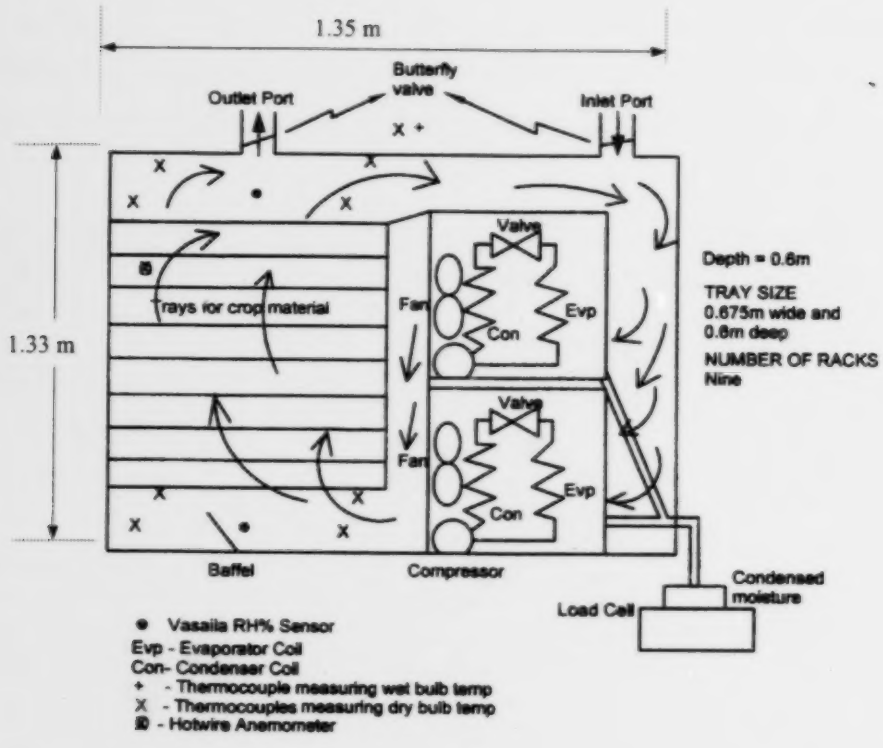

Figure 2. Block diagram of the experimental dehumidifier system showing two dehumidifiers

Table 1. Heat pump dehumidifier specifications (marketed by Canadian Tire Corporation™ Model-43-5404-8 D1)

Refrigerant used	R134a
Power rating	424 W
High side pressure (condenser)	2.03 MPa
Low side pressure (evaporator)	0.97 MPa
Dehumidifying capacity of each heat pump	9.5 L of water per day
Internal fan model no. IS – 4420WCA	1125 rpm

Note: Refer to Appendix A for complete details of the dehumidifiers

3.2 Moving Bed Prototype Heat Pump Dryer

The large scale continuous flow heat pump dryer system is shown in a photograph in Figure 3. It uses re-circulating air as the drying medium. A drying chamber containing a continuous bed conveyor is incorporated into the unit in series with the heat pump system.

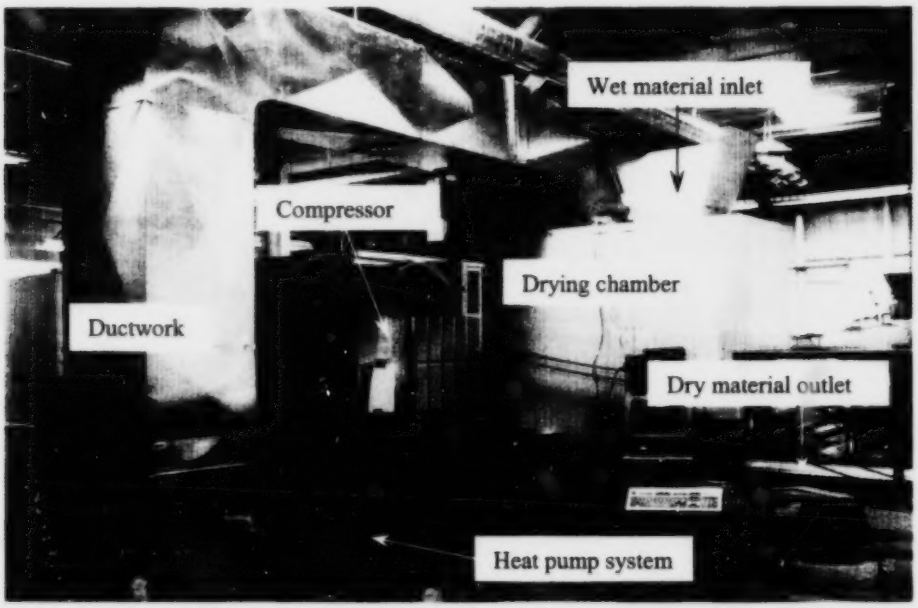

Figure 3. Overview of prototype cross-flow continuous bed heat pump dryer system

The dryer portion of the system consists of three conveyors as shown schematically in Figure 4. Two conveyors (C1 and C2) are used for material drying and the third conveyor (C3) carries the dried material out of the drying chamber. The two conveyors carrying material (C1 and C2) move in opposite directions. The dryer inlet air flows from the bottom to the top of the drying chamber in a cross-flow direction. The dryer dimensions are shown in Figure 4. The airflow rate in the prototype heat pump dryer is assumed constant at 472 L/s (1000 cfm). The diameter of conveyor belt perforations is $1/16^{th}$ of an inch and with a minimum of 30% open area over the entire belt. Dryer frame material is made up of 2 x 2 x 1/8 in^3 hollow structural steel. The conveyor is driven by a 3-phase motor with gear reduction and inverter of 5-50 rev/h. Conveyor material is made up of stainless steel and

food grade plastic. The dryer frame and removable panels are painted with food grade epoxy paint.

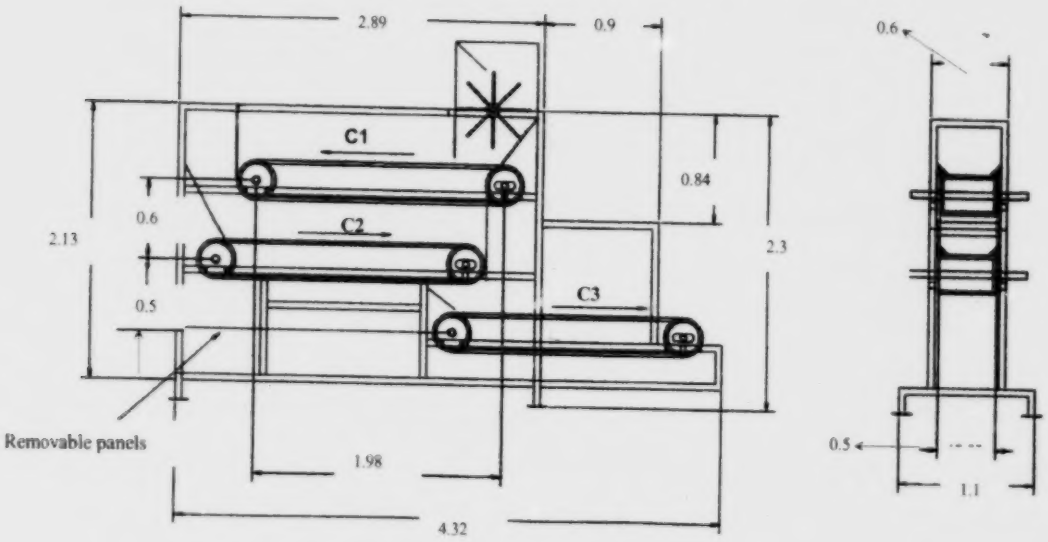

All dimensions are in meters

Figure 4. Schematic sectioned view of the counter cross flow continuous bed drying chamber

Figure 5 is a schematic diagram of the prototype heat pump system. The heat pump system is manufactured by Blanchard-ness, Montreal, QB. The compressor motor has the horse power of 0.5 and runs at 1750 rpm. The refrigerant used in the heat pump system is 404A. This system is designed to operate between high and low refrigerant pressures of 2.86 MPa and 1.48 MPa. The condenser and evaporator coils are made of copper, while the fins attached over these coils are of aluminum. The dimensions for both the coils and thermo-physical properties of refrigerant are provided in Appendix B. The cost of the commercial heat pump system was $15,000. The cost of the dryer system was about $15,000, including the construction costs, which were about $8,000.

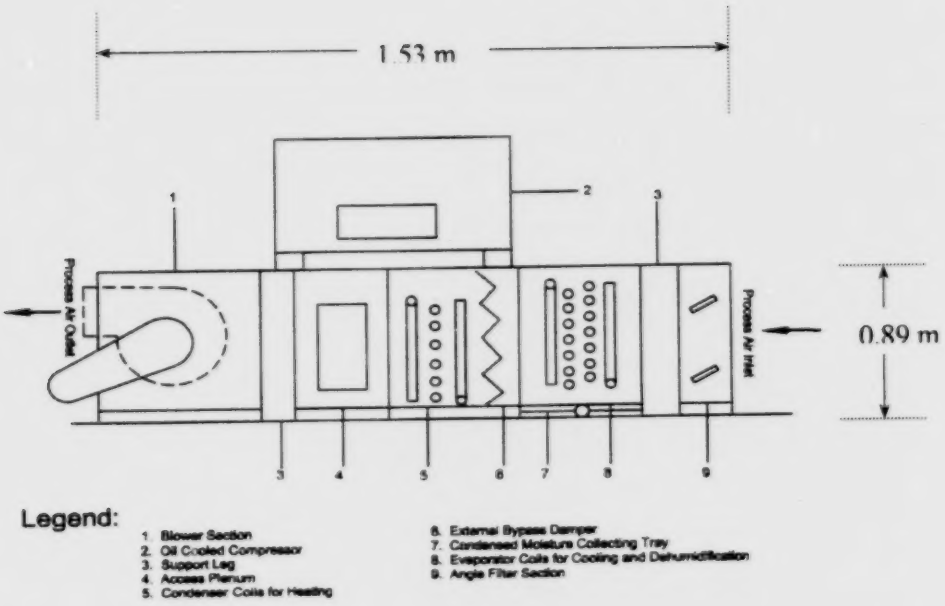

Figure 5. Schematic block diagram of the commercial heat pump system

4. TASK B – Experimental Evaluation of the Cabinet and Continuous Bed Dryers

Experimental evaluation of both the dryers was important in order to understand the drying characteristics of specialty crops and to determine the comparative performance of systems.

4.1 Experimental Evaluation of Cabinet Dryer

This section presents a detailed description of the experimental tests conducted on the cabinet dryer shown previously in Figure 2 (also referred to as setup 2).

4.1.1 Instrumentation

Figure 1 shows the locations where temperature and relative humidity (RH) readings were recorded using a LCD digital hygrometer (Model no. 3309-50, Cole-Parmer Instrument Company, Chicago, IL-60648, USA). Temperature and RH (relative humidity) readings were taken at the entrance and exit of the stacked trays and between the condenser and evaporator coils. Atmospheric temperature and RH values were also measured using this instrument. A hot wire anemometer was used to measure the velocity of process air between trays 4 and 5 (the bottom tray was considered as tray 1). It was assumed that the air velocity would be relatively uniform at that point. The mass of moisture condensed at the evaporator and crop material dried was measured using two electronic weighing scales. All the measurements were taken and recorded manually.

Figure 2 shows the location of thermocouples installed to measure air temperature at the entrance and exit from the stacked trays and in the space between the condenser and evaporator coils in setup 2. Thermocouples were also mounted on the evaporator and condenser coils to measure the pipe surface temperatures. The ambient air relative humidity was measured using the wet bulb and dry bulb temperature sensors. Two RH sensors were located; one at the air entrance and the other at the air exit from the trays to measure the relative humidity. A hot wire anemometer was used to measure the velocity of process air between the trays. The velocity measurements were done in between tray 7 and tray 8 (the

bottom tray was counted as tray 1). It was assumed that the air velocity would be relatively uniform at that point.

Instantaneous power was measured by a wattmeter. The mass of the moisture condensed at the evaporator and crop material dried was measured using a load cell and an electronic weighing scale, respectively. Two ports, one for inlet air and the other for outlet air were made. These ports were used to maintain a constant temperature (steady state condition) inside the drying chamber by periodically opening and closing them. The opening and closing of the inlet and outlet ports at the top of the drying chamber was done manually using butterfly valves. The mass flow rate of air at the inlet port was measured using a Pitot tube. Temperatures, relative humidity and the mass of water condensed were monitored continuously using a data logger. Details of all the instrumentation used are provided in Table 2. Due to the practical difficulties in installing a flow sensor in the heat pump, the measurement of the refrigerant mass flow rate was not done. The refrigerant mass flow rate was calculated as a part of a larger simulation model (Adapa, 2001).

Table 2. Instrumentation used in the tests for the second setup

	Instrument	Manufacturer	Range	Calibrated range	Uncertainty
1)	T-type Thermocouples	Omega Engineering Inc.	-60°C to 100°C	0°C to 100°C	±1°C
2)	Relative Humidity sensors	Vaisala (HMP233)	0% to 100% RH	5% to 95% RH	±0.95% RH
3)	Hotwire Anemometer	TSI Incorporation (VelociCalc)	0 to 50 m/s	0 to 50 m/s	0.015 m/s
4)	Pitot tube	Air Flow Development	0.33 to 1.65 m/s	0.33 to 1.65 m/s	±0.013
5)	Data logger	Sciemetric Instrument (8082A)	0-5 V	N.A.*	N.A.
6)	Wattmeter	Valhalla Scientific (Model no. 2101/3 - 8113)	N.A.	N.A.	N.A.

*Not Applicable

4.1.2 Experimental Procedure

Experiments were performed with fixed tray and moving tray drying. The alfalfa was chopped to a size of 50 mm. Using an electronic balance, 0.14 kg and 0.40 kg of alfalfa was

weighed and spread uniformly over trays for setup 1 and setup 2, respectively. The thickness of the layer was 20-30 mm. The initial moisture content of alfalfa was 70% (wet basis), which was determined following the ASAE Standard S358 (ASAE, 2000) for moisture content measurement.

Three fixed tray/batch drying experiments were performed for setup 2. In fixed tray drying, nine trays were placed in the drying chamber at the beginning of the experiment and the doors were closed. The material in each tray was weighed at 30 min time intervals. This was done by rapidly removing the trays from the cabinet, weighing them on an electronic scale and returning them back to the cabinet. Moisture content at each weighing interval was calculated from the initial moisture content of alfalfa and the mass loss from each tray. The fixed tray drying continued until the moisture content of the material in all the trays was lower than 10% (wet basis).

Three moving tray-drying experiments were performed setup 2. Moving tray drying experiments were conducted immediately following the batch/fixed tray drying. This was done because the system was at steady state at the end of the fixed tray drying period. Nine fresh trays of alfalfa were placed in the chamber at the beginning of fixed tray drying. Drying was continued until the bottom tray (tray 1) reached 16% moisture content. Tray 1 was removed from the chamber, all other upper trays were moved down on the racks and a fresh tray of material was placed on the top rack. The door was closed and the material in all the trays was dried for another 30 min. The entire set of trays were removed rapidly from the cabinet and weighed. When the bottom tray reached near 10% moisture content, the removal and weighing were repeated. This procedure was repeated until the 18^{th} tray had been reached to the bottom and it dried to below 10% moisture content. At this point the drying experiment ended.

4.1.3 Results and Discussion

A combination of two drying configurations (fixed tray or moving tray) were tested. Each combination was repeated three times for a total of 6 experiments listed in Table 3. The

total number of trays passed through the system for each test is listed. The total mass is the cumulative mass of alfalfa on all trays before and after drying. The average mass of alfalfa on each tray was about 400 g.

Table 3. Summary of data from experimental drying of alfalfa chops in a re-circulating air cabinet using household dehumidifiers.

Test no.	Drying configuration	No. of dehumidifier	No. of trays	Mass of alfalfa tested (kg)		Moisture content (%)		Drying time (min)	Instantaneous power consumption (W)	Temp (°C)		RH (%)		Drying air velocity (m/s)	Mass of condensed water (kg)
				Initial	Final	Initial	Final			Max	Min	Max	Min		
1	fixed tray	2	9	3.60	1.18	70.0	8.5	311	428	51.1	24.1	80.5	20.4	0.36	1.279
2	fixed tray	2	9	3.60	1.52	65.1	17.3	300	413	40.1	19.2	71.1	20.5	0.37	0.666
3	fixed tray	2	9	3.60	1.41	65.0	10.6	330	415	40.2	18.4	72.0	21.2	0.38	1.122
4	fixed followed by moving tray	2	27	10.80	3.86	69.0	13.3	780	423	46.8	20.1	77.1	19.8	0.36	3.413
5	fixed followed by moving tray	2	27	10.80	3.80	68.4	10.1	780	424	47.0	19.8	78.0	20.0	0.37	3.305
6	fixed followed by moving tray	2	27	10.80	3.94	68.8	14.5	780	423	46.2	20.0	77.4	21.3	0.36	3.613

*Not measured

The initial moisture content of alfalfa chops ranged from 65% to 71%. The final moisture content varied from one test to the next. The drying times listed in Table 3 represent the total drying time. The instantaneous power consumption recorded in setup 2 ranged from 413-428 W. The minimum temperature represents the ambient temperatures during a test, averaged 20°C.

The mass of condensed water was almost half of the total mass of water lost from alfalfa. The other half likely leaked to the outside during opening and closing the door. This is evident from a larger mass of water condensed in the fixed tray configuration than in moving tray configuration.

Preliminary data was collected using setup 1 which was not fully instrumented. These initial experiments provided a basic understanding of the process. In setup 2, which was fully instrumented, moving tray drying experiments were performed immediately following the fixed tray drying test. The results obtained from the moving tray-drying experiments in setup 2 are discussed in the remainder of this paper. These results are a representation of both fixed and moving tray drying experiments.

Figure 6 shows the temperature and relative humidity of the air as the material dried. The air temperature at the inlet and outlet of the drying section increased and reached nearly constant values. Initially, the temperature was low because the material was wet and cool. As time progressed, the material was heated and drying commenced. The maximum temperature at the entrance to the trays was 45°C. The temperature was maintained at 45°C by opening and closing the inlet and outlet butterfly valves manually (Figure 2). There were two reasons for not allowing the temperature to exceed 45°C. First reason was that for specialty crops the optimum drying temperatures (at which no structural damage and nutrient losses occurs) stated to lie between 30-45°C. The second reason was that when temperatures of process air increased above 45°C, the energy required to condense moisture at the evaporator increases.

The relative humidity of air at the entrance and exit of the trays decreased almost exponentially from an initial value of 79% down to 19% by the end of fixed tray drying (Figure 6). The initial high moisture content of the material and low temperature of air resulted in high air relative humidity values. The air became drier due to the onset of the falling drying rate characteristics.

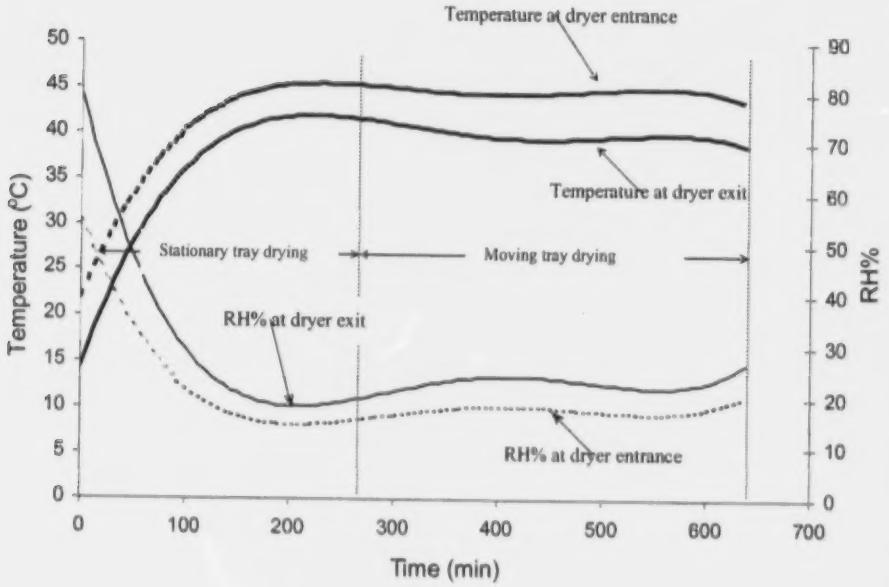

Figure 6. Typical measured temperature and relative humidity of air at the dryer entrance and exit for experiment number 12

The emulation of continuous flow (moving tray) drying was initiated after 270 minutes of fixed tray drying. During the moving tray tests, temperature and relative humidity were constant because, on an average, the moisture loading of the material in the test chamber was also constant. As the moving tray drying started, the relative humidity at the exit of trays, which was below 20%, increased and reached 30% and remained constant thereafter. Fresh material was introduced into the dryer every 30 min and dry material was removed maintaining a near steady rate of moisture evaporation.

Figure 7 shows cumulative moisture condensation for fixed tray drying followed by moving tray drying. The initial moisture condensation was high for fixed tray drying and decreased

as the drying progressed, reaching almost zero at about 270 min (end of fixed tray drying). As the relative humidity of air decreased, condensation rate decreased as well diminishing completely at relative humidity values below 20%. In the moving tray mode, fresh moist material was introduced every 30 min, which increased the relative humidity of the air (to about 30%). The result was an initial increase in the condensation rate followed by a constant rate of condensation. The amount of moisture condensed at the evaporator was approximately 50% of the total moisture evaporated from the alfalfa. The remaining 50% of the moisture was mainly lost to the ambient air through inlet and outlet ports, with some additional loss occurring when the chamber door was opened to introduce fresh alfalfa and remove dried alfalfa.

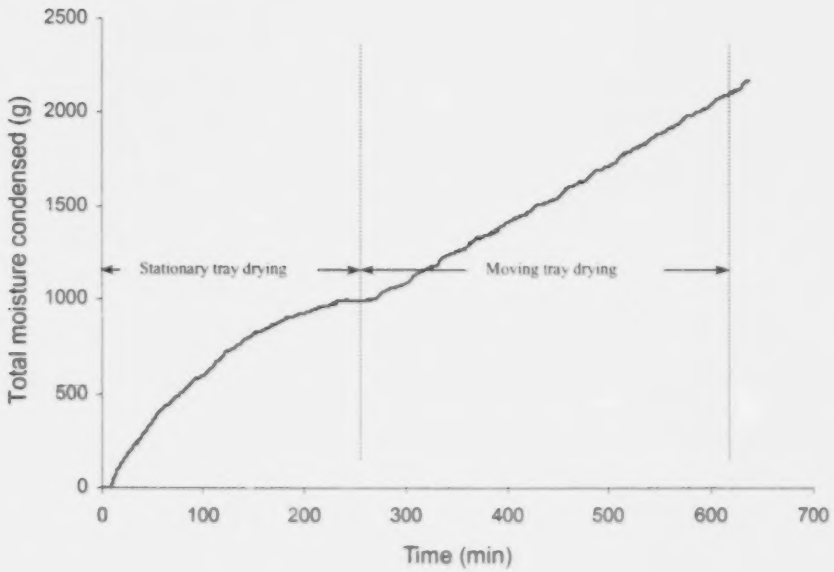

Figure 7. Typical measured moisture condensation during fixed and moving tray drying with time for experiment number 12

Figure 8 shows the measured specific moisture extraction rate (SMER) and instantaneous power consumed during the drying process. SMER is defined as the mass of water removed per unit of energy expended. The high SMER of 1.02 kg/kWh in the first 40 min was due to the high moisture condensation rate (0.45 kg/h) and low power consumption. After 40 min, a decreasing trend in SMER and the relative humidity of the air was observed. As the

moving tray drying method started, the SMER increased to an average of about 0.5 kg/kWh and remained steady at this value throughout the remainder of the test. In moving tray drying, the relative humidity of process air was about 30%. Previous research (Clements, 1993; Prasertsan and Saen-Saby, 1998; Tai et al., 1982; Theerakulpisut, 1990) suggests that a heat pump system is more efficient when it is run at 30% or higher relative humidity of process air entering the evaporator coil, enabling a high degree of condensation. As the material mass flow rate through the dryer increases, the relative humidity of the air is also increased leading to a higher value of SMER (Clements et al., 1993).

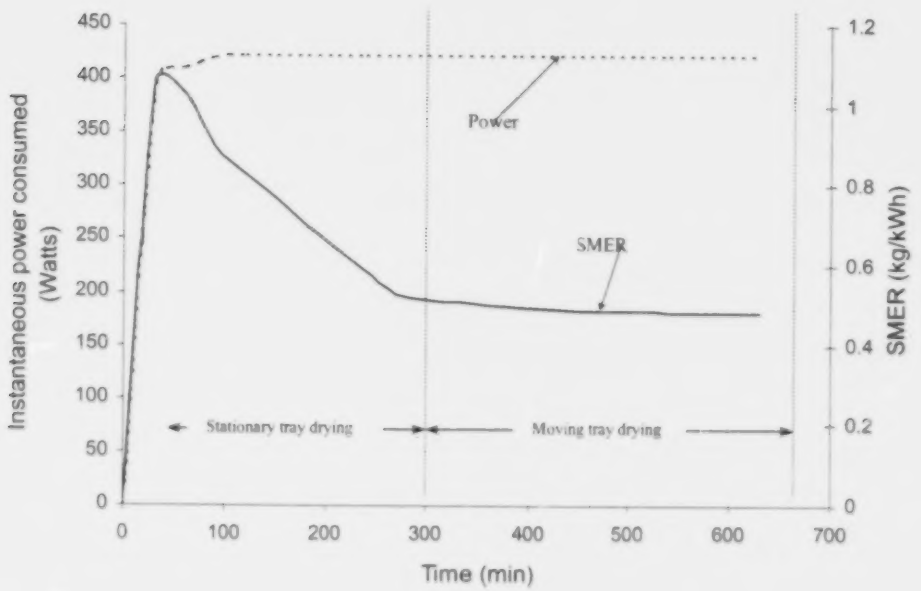

Figure 8. Specific moisture extraction rate and instantaneous power consumed by heat pumps over the drying process for experiment number 12

The SMER values obtained are about $1/3^{rd}$ of previously published results (Clements et al., 1993). We can think of three reasons for deviation of our data from previously published SMER values: (1) the evaporator and condenser coils of household dehumidifiers were not effective in cooling or heating the air near to refrigerant temperatures; (2) drying rate of a hygroscopic alfalfa is lesser than that for non-agricultural material (sponge, lenin cloth, etc.) used by other researchers; and (3) maintaining a constant temperature inside drying

chamber, by exhausting portion of the air from the cabinet, resulted in loss of latent and sensible heat.

The initial instantaneous power consumed was low due to the low temperature of air at the exit from condenser. This is because the power consumption by the compressor of a heat pump depends on the temperature of refrigerant. If the temperature of refrigerant is low then the power consumed by compressor will be low. Therefore, power consumption increased over time as drying progressed because the latent heat released by the material resulted in an increase in refrigerant temperature.

Figure 9 shows the variation in moisture content of alfalfa for individual trays. The first nine trays were batch (fixed tray) dried. The resulting drying curves for the first nine trays had a similar pattern (only curves for trays 1 and 9 are shown). After 270 min, when a fresh tray of material entered the chamber, it was noted that the slope of the curves became steep. The air temperature at the beginning of fixed tray drying was low (approx. 22°C). It increased gradually as drying progressed until it reached a plateau of 45°C. This led to an increase in moisture removal rate from alfalfa during moving tray drying, resulting in parallel curves. For the same amount of material, fixed tray drying took about 5 hours while the moving tray drying took 4 hours to dry the material (Table 3).

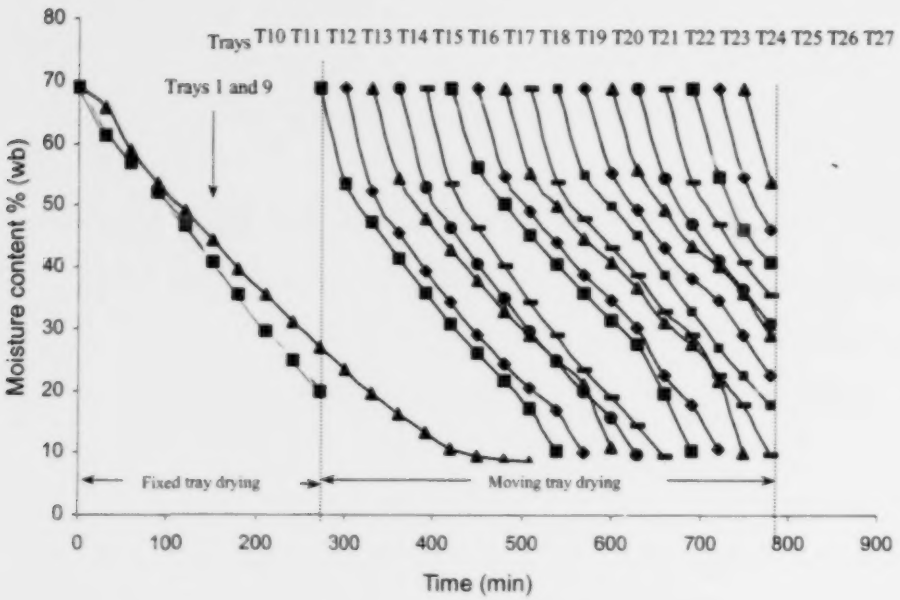

Figure 9. Typical moisture content of material in individual trays over drying time for experiment number 12

4.1.3.1 Energy and Mass Balance

Energy Balance

During the experiments, the inlet and outlet ports at the top of drying chamber were opened occasionally in order to maintain a constant temperature (45°C) at the condenser exit. This process was achieved by allowing relatively cold ambient air to mix with hot process air at the inlet port while discharging an equal amount to atmosphere at the outlet port (Figure 2). The instantaneous energy supplied to the dryer (q_i) will be the difference in energy gained by the re-circulating air at the condenser coil to that of energy recovered by the evaporator coil from the re-circulating air at the dryer outlet. The instantaneous energy loss (q_l) by the system through outlet port was determined by calculating the difference in energy of re-circulating air at the dryer exit to that of energy of re-circulating air at the evaporator entrance (after mixing, re-circulating and ambient air at inlet port). The instantaneous energy supplied and energy lost by the system can be determined as follows (refer to Table 4 for calculations):

$$q_i = m_{ad}\ C_{pa}\ (T_1 - T_4) \quad (1)$$

$$q_l = m_{aa}\ C_{pa}\ (T_2 - T_a) \quad (2)$$

Where, m_{ad} and m_{aa} are the mass flow rates of air inside the drying system and mass flow rate of ambient air entering the system, respectively. Mass flow rates were determined by calculating the product of air density, cross-sectional area and air velocity. m_{ad} was calculated by using cross-sectional area of the column of stacked trays and average air velocity, while m_{aa} was determined by using cross-sectional area of the inlet port and ambient air velocity through it. C_{pa} is specific heat of air. T_1, T_2 and T_4 are process air temperatures at dryer inlet, dryer outlet and condenser inlet. T_a is outside air temperature. Table 4 indicates that about 25% of the heat was lost to the ambient air through the inlet and outlet ports.

Table 4. Calculations for energy balance

m_{ad} (kg/s)	m_{aa} (kg/s)	C_{pa} (kJ/kg-K)	T_1 (K)	T_2 (K)	T_4 (K)	$T_{ambient}$ (K)	q_i (J/s)	q_l (J/s)
0.1539	0.1125	1.008	318	313	288	297	4653.94	1814.40

Mass Balance

As explained earlier, the inlet and outlet ports at the top of drying chamber were opened occasionally in order to maintain a constant temperature (45°C) at the condenser exit. This process was achieved by allowing relatively dry outside air to mix with humid air inside (Figure 2). The moisture extracted from alfalfa at any instance (m_t) will be the difference in moisture content of re-circulating air at the dryer exit and that of at the dryer inlet. The instantaneous moisture lost (m_l) by the system at the outlet port was determined by finding the difference between moisture content of re-circulating air at dryer exit and the air at the evaporator inlet. The instantaneous moisture extracted from alfalfa and the moisture lost by

the system can be determined from the following equations (refer to Table 5 for calculations):

$$m_i = m_{ad}(W_2 - W_1) \tag{3}$$

$$m_l = (m_{ad} - m_{aa})(W_2 - W_3) \tag{4}$$

$$W_3 = \frac{(m_{ad} - m_{aa})W_2 + m_{aa}W_a}{m_{ad}} \tag{5}$$

Where, W_1, W_2 and W_3 are humidity ratios of air at dryer inlet, dryer outlet and at evaporator entrance, respectively. W_a is the ambient air humidity ratio. The mass flow rates of air inside the chamber (m_{ad}) and the ambient air entering the drying chamber (m_{aa}) were calculated following the same procedure as outlined in the previous section on energy balance.

Table 5. Calculations for mass balance

m_{ad} (kg/s)	m_{aa} (kg/s)	W_1 (g/kg)	W_2 (g/kg)	W_3 (g/kg)	$W_{ambient}$ (g/kg)	m_i (kg/h)	m_l (kg/h)
0.1539	0.1125	10.00	11.50	7.11	5.50	0.831	0.654

4.1.3.2 Measured Psychrometric Conditions of Process Air

Figure 10 shows the psychrometric process for drying for one air cycle through the dryer and heat pump. This figure represents a particular set of drying conditions inside the chamber at the beginning of fixed tray drying. In Figure 10, the path from 1 to 2 represents the drying process. Points 1 and 2 are the conditions of process air at the dryer entrance and exit, respectively. The drying of agricultural material is often considered to be an adiabatic process (Sosle et al., 2000). The experimental results suggest that the drying process 1 - 2 was not adiabatic, even though the chamber was well sealed and insulated from surroundings. For the drying process to be adiabatic, it is essential to have availability of

free moisture in the drying chamber. However, crop materials often do not have most of their moisture content on the surface. Therefore it takes extra energy to drive the moisture from the core of crop material.

As represented by the process 2 – 3 – 4 – 4' in Figure 10, the evaporator coil was ineffective in cooling all of the process air close to the coil temperature. One reason for the ineffectiveness of the coils was the absence of fins, thus increasing the "effective" bypass of air not in contact with the coils. The fraction of air bypassed through the evaporator 'b' can be determined from (McQuiston and Parker, 1998)

$$b = \frac{T_{4'} - T_4}{T_2 - T_4}. \tag{6}$$

This bypass factor provides an indirect measure of the efficiency of heat transfer at the coils. From the psychrometrics of Figure 10, b was calculated to be 0.71. The value of b for an efficient process at the evaporator should be in the range of 0.1 to 0.15 (McQuiston and Parker, 1998).

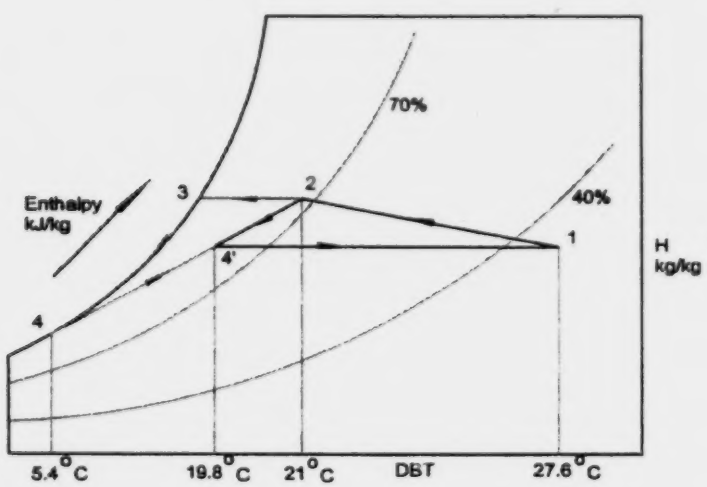

Figure 10. Measured psychrometric condition of process air with air bypass around evaporator coils and non-adiabatic drying

4.2 Experimental Evaluation of Prototype Heat Pump Dryer

This section presents the experimental results obtained on the prototype commercial or large scale heat pump drying system.

4.2.1 Instrumentation

Figure 11 shows the location of all instrumentation installed in the prototype heat pump dryer system. Type T Thermocouples were used to measure air temperatures at the inlet and exit of the drying chamber, at the inlet of evaporator coil and between the evaporator and condenser coils. Thermocouples were also mounted on the evaporator and condenser coils to measure the refrigerant temperatures. The ambient air relative humidity (RH) was determined using the wet bulb and dry bulb temperature measurement.

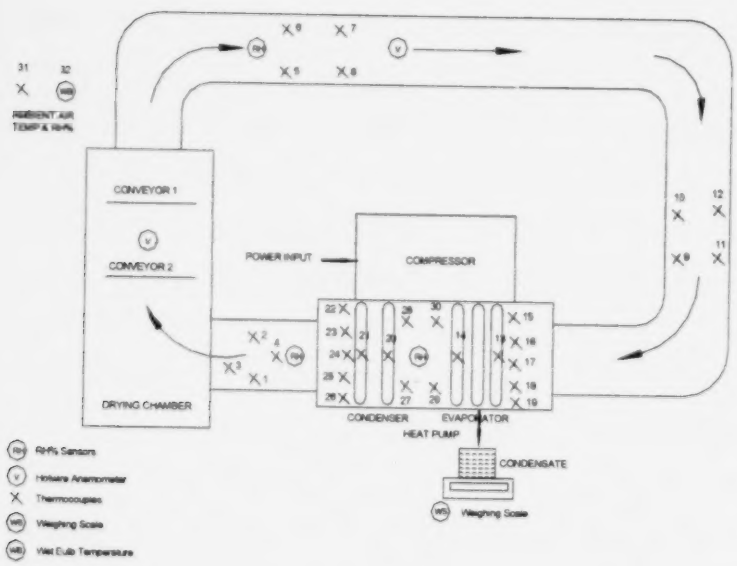

Figure 11. Block diagram of prototype heat pump dryer system depicting the locations of instrumentation

Three relative humidity sensors were installed; one at the entrance, one at the exit of dryer and one in the space between condenser and evaporator coils. A hotwire anemometer

located between conveyors 1 and 2 was used to measure the air velocity in the closed loop system.

The mass of the moisture condensed at the evaporator and crop material dried was measured using a load cell and an electronic weighing scale, respectively. The temperatures, relative humidities and the mass of water condensed were monitored online using a data logger. Details of all the instruments are provided in Table 6.

Table 6. Instrumentation used in the tests on the prototype heat pump dryer

	Instrument	Manufacturer	Range	Calibrated range	Uncertainty
1)	Type T Thermocouples	Omega Engineering Inc.	-60°C to 100°C	0°C to 100°C	±1°C
2)	Relative Humidity sensors	Vaisala (HMP233)	0% to 100% RH	5% to 95% RH	±0.95% RH
3)	Hotwire Anemometer	TSI Incorporation (VelociCalc)	0 to 50 m/s	0 to 50 m/s	0.015 m/s
4)	Data Logger	Sciemetric Instrument (8082A)	0 – 5 V	N.A.*	N.A.

* Not Applicable

A thermostat and a humidity sensor were built into the heat pump system. The thermostat helped to maintain a constant temperature of air at the condenser outlet (dryer inlet), while the humidity sensor was used to check the relative humidity of air entering the evaporator. The system is designed to operate between user specified limits of temperature and relative humidity.

4.2.2 Determination of Material Moisture Content

Prior to all drying experiments, the initial moisture content of material was determined. The moisture content was calculated according to the procedure of ASAE Standard S358 (ASAE, 2000). The parameters involved and results are provided in Table 7.

Table 7. Material initial moisture content determination.

	Material	Oven temperature (°C)	Initial weight (g)	Final weight (g)	Drying time (h)	Initial moisture content (%)
1)	$Alfalfa_c$	103.0	25.0	8.2	24.0	67.0
2)	$Catnip_c$	103.0	25.0	7.5	24.0	69.9
3)	$Wormwood_c$	103.0	25.0	9.3	24.0	62.7
4)	$Red\ Clover_c$	103.0	25.0	8.9	24.0	64.6
5)	$Portulaca_c$	103.0	25.0	2.6	24.0	89.6
6)	$Alfalfa_w$	103.0	25.0	3.5	24.0	77.7
7)	$Red\ Clover_w$	103.0	25.0	3.4	24.0	77.5
8)	$Carrot_s$	100.0	10.0	1.3	1.7	87.5
9)	$Carrot_w$	100.0	10.0	1.2	1.7	88.3
10)	$Dandelion_w$	100.0	10.0	3.1	1.7	68.9
11)	$Ginseng_w$	100.0	10.0	3.2	1.7	68.2

c, s and w stands for chopped, sliced and whole, aerial and root crops.

4.2.3 Preliminary Experimental Results

Five preliminary drying experiments were performed using alfalfa chops to find the approximate speed of conveyor belts, such that fresh material introduced onto the top (conveyor 1) will dry to a moisture content of less than 10% at the dryer exit (refer to Table 8). In the first two experiments, one-year-old refrigerated alfalfa chops were used since fresh cut alfalfa was not available. These chops were defrosted to near room temperature before the drying started. In the next three experiments fresh alfalfa chops were dried. It was found that for the same material flow rate and drying air temperatures, defrosted alfalfa chops dried faster than the fresh chops. The reason could be that at lower temperatures (-25°C to -30°C) the moisture at the core of material diffuses slowly towards material surface, due to the difference in moisture concentration. The moisture on the material surface freezes when it comes in contact with very low temperatures. When frozen material is defrosted at room temperature (prior to drying), the availability of free surface moisture increases, which in turn enhances the drying rate of material. To get a final moisture content of 10% (wb), the material flow rate for fresh chops had to be lowered compared to the values used for defrosted chops (Table 8). A known amount of mass of material on the conveyors was weighed at the exit of drying chamber to determine the final moisture content. From Table 8, it is apparent that a flow rate of about 2.9 kg/h of alfalfa will result in alfalfa leaving the dryer close to the desired moisture content.

Table 8. Results of preliminary alfalfa drying experiments

	Drying air temperatures (°C)	Initial moisture content (%)	Final moisture content (%)	Drying time (h)	Air velocity (m/s)	Material flow rate (kg/h)	Material bed thickness (m)
1(defrosted)	30.0	72.3	4.4	3.5	2.2	3.4	0.03
2(defrosted)	30.0	67.3	3.1	4.0	2.2	3.0	0.03
3(fresh)	30.0	68.8	15.0	4.0	2.1	3.0	0.03
4(fresh)	30.0	67.0	10.4	3.3	2.1	2.9	0.03
5(fresh)	30.0	65.7	4.2	4.5	2.1	2.6	0.03

It was expected that most of the specialty crops consisting of leaf and stem material (catnip, wormwood, red clover, etc.) would have drying characteristics similar to alfalfa. However, root crops such as ginseng, dandelion, etc., are likely to take significantly longer time to dry because of their low surface area to mass ratio. Some experimental tests were conducted on carrots because they were readily available and inexpensive. Drying rate was comparatively so slow that they could be as effectively dried in batches (i.e. static bed or conveyors not moving).

4.2.4 Experimental Results for Several Crop Materials

For comparative purposes, experimental tests were conducted using the prototype heat pump dryer for a range of crops based on their availability and cost. With the exception of carrots, all of these crops (including alfalfa) are being marketed or are under development (portulaca and dandelion roots) as herbal type medicines.

Only one drying experiment was performed on catnip, wormwood, red clover chops and whole aerial parts of red clover. This was due to the limited availability of material. These materials were provided by Dr. Branka Barl of Crop Science Department, University of Saskatchewan from her research fields. The availability of dandelion roots was also limited and not considered of enough interest to warrant more than one test. They were acquired from Ms. Wanda Wolf (Lonewolf Herbal Resources, Phippen, SK).

A single drying experiment on the ginseng roots was also conducted. Here the cost of ginseng roots was the constraint. The roots were bought from Mr. Charles Chernak (CSI Ginseng Products, Delhi, Ontario). The unwashed roots after harvest were shipped to the University of Saskatchewan and received after about four days. The roots were than stored in a refrigerator at 4°C for couple of days prior to drying.

Two batches of carrots were dried, one sliced and one whole. Sliced carrots have a much higher surface area to mass ratio and should dry much quicker. This may be an option that growers could choose to exercise for some root crops. The slices were 4 mm thick.

The chopped aerial crops and sliced carrots utilized continuous drying, while whole aerial (alfalfa and red clover) and root crops, were dried using static bed or batch process. In continuous bed drying the material was introduced at one end of conveyor 1 and spread uniformly over the length and width of the belt. The feed rate of material was adjusted to match the conveyor belt speed. The density and moisture content of chopped leaf and stem material was approximately 187 kg/m^3 and 70%, respectively.

In static bed drying the material was uniformly spread over the conveyors 1 and 2 at the beginning of experiment. A portion of known mass of material at the center of conveyor 2 was monitored manually to check the moisture content after every 12 hours. The drying was stopped when the average moisture content of material dropped below 10%. The mass flow rate of air inside the duct system was maintained at close to 86 kg/m^2-min (1000 cfm) generating a drying air velocity that varied from 1.6 m/s to 2.2 m/s.

The whole aerial and root crops were dried at 35°C while the chopped aerial material was dried at 30°C. The temperature was maintained above 30°C because some research studies in the past have suggested that temperatures below 30°C can result in mold growth during drying. Drying temperatures above 38°C may result in an undesirable brown color (van Dalfsen et. al, 1992; van Hooren and Lester, 1991). If there was a concern about quality, temperatures of 30°C could still likely be used with the heat pump system because of the expected shorter drying times.

Table 9 shows drying properties of various specialty crop materials. The first seven crops fall under the category of the leaf and stem (aerial) type. They were segregated into chopped and whole aerial crops. The chopped aerial crops were dried at an average temperature of 30°C, as were the sliced carrots, while whole aerial crops were dried at 35°C. For the same material flow rate and drying time, the final moisture content of chopped catnip was found to be lowest (5.1%), while for chopped alfalfa, wormwood and red clover, it was in the range of 9.5±0.8%. The higher drying rate of catnip could be due to comparatively bigger pores on its leaves and stems, which helped moisture to escape more readily, compared to other material. Chopped portulaca on the other hand dried almost three times slower than other chopped aerial crops (alfalfa, catnip, wormwood and red clover). This was due to high moisture content and sticky nature of chopped aerial parts of portulaca, which caked while drying and did not allow hot and dry air to pass through, exposing less surface area for drying. The chopped material was uniformly spread on the conveyors. The average thickness of the material bed was maintained at 30 mm, such that the drying will follow a thin-layer drying pattern. It was also observed from Table 9 that chopped aerial crops dried almost seven times faster than whole aerial parts (alfalfa and red clover). This is likely due to lower surface area to mass ratio of whole aerial crops.

Table 9. Drying characteristics for several leaf-stem (aerial) and root type crops

	Material	Drying temperature (°C)	Initial moisture content (%)	Final moisture content (%)	Drying time (h)	Air velocity (m/s)	Total mass of material (kg)	Material flow rate (kg/h)	Material bed thickness (m)
1)	$Alfalfa_c$	30.0	67.0	10.4	3.3	2.1	N.A.*	2.9	0.03
2)	$Catnip_c$	30.0	69.9	5.1	3.3	2.0	N.A.	2.9	0.03
3)	$Wormwood_c$	30.0	62.7	8.9	3.3	2.2	N.A.	2.9	0.03
4)	$Red\ Clover_c$	30.0	64.6	9.3	3.3	2.0	N.A.	2.9	0.03
5)	$Portulaca_c$	35.0	89.6	10.8	9.6	1.7	13.2	N.A.	0.03
6)	$Alfalfa_w$	35.0	77.7	10.3	21.5	1.6	17.4	N.A.	N.A.
7)	$Red\ Clover_w$	35.0	77.5	9.4	22.8	1.6	11.6	N.A.	N.A.
8)	$Carrot_s$	30.0	87.5	6.7	6.1	2.1	N.A.	1.9	0.004
9)	$Carrot_w$	35.0	88.3	7.1	81.0	1.9	20.7	N.A.	N.A.
10)	$Dandelion_w$	35.0	68.9	7.4	53.0	1.9	18.4	N.A.	N.A.
11)	$Ginseng_w$	35.0	68.2	6.8	120.0	1.9	20.6	N.A.	N.A.

c, s and w stands for chopped, sliced and whole, aerial and root crops; * Not applicable

The whole roots dried at a much slower rate than the chopped aerial components (16 to 36 times slower). The average initial moisture content of roots was about 69% with carrot as the exception at 88% moisture content. The whole roots were dried at an average temperature of 35°C. In static bed drying, a portion of known mass of material at the center of conveyor 2 was monitored manually to check the moisture content every 12 hours. Figure 12 shows the variation in material moisture content over drying period for three root crops. A close look at Figure 12 shows that the drying rate for carrot and dandelion are nearly identical (i.e. they have approximately same slope). If initial moisture content were the same, curves would have been similar. Ginseng, however, has a much lower slope.

It was found that the drying time for all the three root types was different. The difference was primarily due to their initial moisture content and physical structure. Dandelion had the fastest drying time as it took only 53 hours to dry (drying started at a much lower moisture content compared to carrots). Carrots had the next highest drying time of 81 hours and finally ginseng, which took about 120 hours to dry. It was observed that ginseng root was composed of two layers. The outer layer dried quickly and shrunk to form a hard and thick layer. This layer significantly reduced moisture diffusion from inside of the root to ambient air. A similar observation was reported by Sokhansanj et al. (1999). They concluded from their study that the skin (epidermis) of ginseng root acts as a major barrier against moisture efflux from the core of the root. It should be noted that the average moisture content for ginseng was reduced below 10% in 5 days (60 hours). However, there was not a uniform distribution of moisture content within the larger roots, at this stage. It was observed that the core of few thick roots did not dry well and needed to be kept in the dryer for another 5 days. After analyzing the drying results for ginseng, it was concluded that it could be best to dry thin and thick roots separately. Adopting this procedure would reduce the drying cost incurred and will increase the productivity of the dryer system. This observation agrees with the conclusions deduced by van Dalfsen et al. (1992) in their forced air dryer system.

The reduction in drying time by slicing root crops is dramatic. Sliced carrots dried about 13 times faster than whole carrots and at a rate of 4 times faster than whole aerials. Slicing root crops prior to drying is recommended.

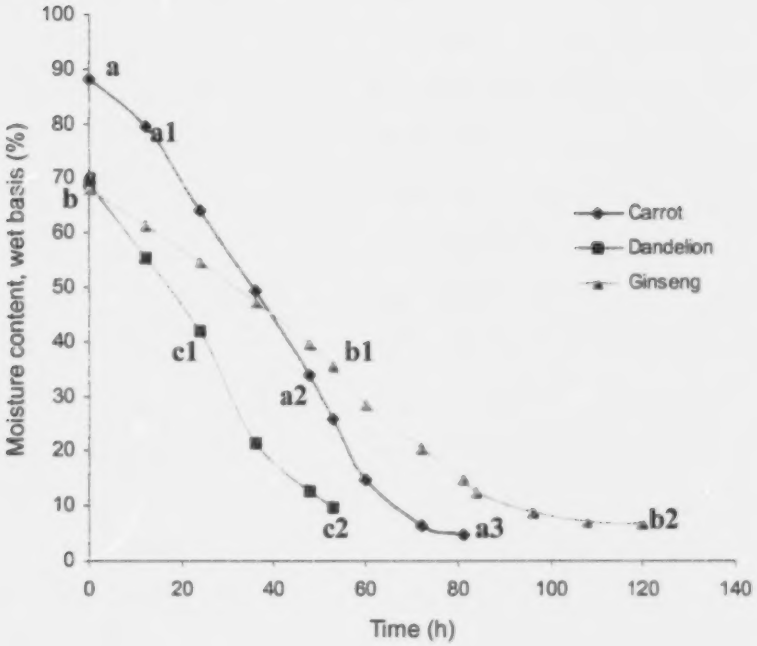

Figure 12. Change in moisture content of different roots over drying time

Photographs of the root material before and after drying are shown in Figures 13 to 19. The dried product for the leaf and stem material looked almost like fresh material. The change in color of the dried product was observed to be negligible when inspected with the naked eye. Similar results were reported by Sosle et al. (2000) where the final product quality in terms of consumer preference was found to be excellent when the drying was conducted at temperatures near 30°C and 35°C. These products showed greater browning and shriveling when dried at higher temperatures (80°C to 100°C). The chewability and mouth feel of the material was superior for the low temperature processed product.

Figure 13. Fresh dandelion roots

Figure 14. Dried dandelion roots

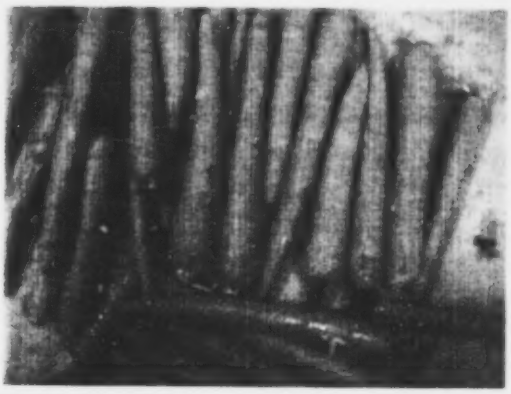

Figure 15. Fresh carrots

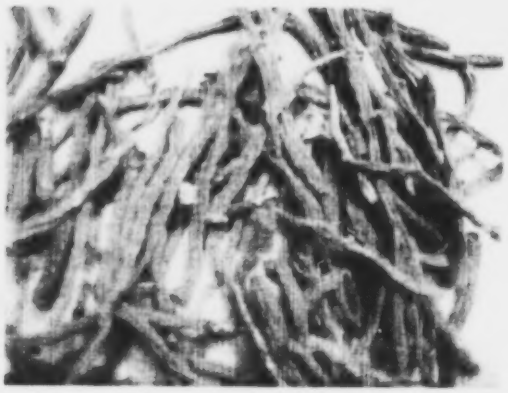

Figure 16. Dried carrots

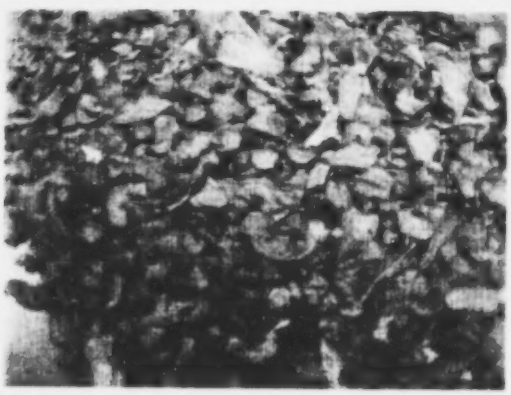

Figure 17. Dried carrots (sliced)

Figure 18. Fresh ginseng roots

Figure 19. Dried ginseng roots

4.2.5 Energy Calculations

It was very important to do energy calculations on the continuous bed prototype heat pump dryer system in order to verify its viability in comparison to the conventional dryers. The primary step was to calculate the total energy supplied by the heat pump to the dryer. The total energy supplied to the dryer will be the difference in energy gained by the re-circulating air at the condenser coil to that of energy recovered by the evaporator coil from the re-circulating air at the dryer outlet. In addition to this, the energy consumed by the blower/fan to circulate air through the system was also included. The commercial heat pump used in the prototype dryer had a built-in thermostat, which helped to maintain a constant temperature of air at the condenser exit (inlet to dryer). Whenever the temperature of air exceeded the specified value, thermostat shut down the heat pump temporarily. It was observed that the system was idle for about 15% of the total drying time. Therefore, a factor of 0.85 was multiplied to the difference in energy supplied by the condenser coil to that recovered at the evaporator coil. The results of energy calculations are provided in Table 10. The following equations were used to perform these energy calculations:

$$Q_{total} = (0.85 * (q_{cond} - q_{evp}) + q_{fan}) * t_t \quad (7)$$

$$q_{cond} - q_{evp} = m_{ad} * C_{pa} (T_1 - T_2) \quad (8)$$

where, m_{ad} is the mass flow rates of air inside the duct system, Q_{total}, q_{fan}, q_{cond} and q_{evp} are total energy supplied to the system fan power, latent heat supplied by condenser and heat recovered (latent and sensible) at the evaporator, respectively. C_{pa} and t_t are the specific heat of air and total time taken by the material to dry. T_1 and T_2 are process air temperatures at dryer inlet and dryer outlet

The psychrometric properties of prototype heat pump dryer system are given in Table 10. These properties were used in the energy calculations and are used in later sections to verify the simulation model of the prototype heat pump dryer. It was noticed that the difference between air temperature at the dryer exit and at the evaporator entrance was negligible. From this it can be concluded that there was negligible energy loss in the duct system.

Table 10. Calculations for energy balance of the prototype heat pump dryer for a mass flow rate of air, (m_{ad}) 1.8 kg/s and fan power (q_{fan}) 373.0 J/s.

	Material	Air temperature at dryer entrance, T1 (°C)	Air temperature at dryer exit, T2 (°C)	Air Relative humidity at dryer entrance (%)	Air Relative humidity at dryer exit (%)	Material drying time (h)	Q_{total} (kWh)
1)	$Alfalfa_c$	30.0	28.1	17.8	25.0	3.3	10.1
2)	$Catnip_c$	30.0	28.0	17.6	24.5	3.3	10.1
3)	$Wormwood_c$	30.0	28.2	16.5	19.9	3.3	10.1
4)	$Red\ Clover_c$	30.0	28.1	16.2	20.1	3.3	10.1
5)	$Portulaca_c$	35.0	33.8	15.1	17.0	9.6	21.4
6)	$Alfalfa_w$	35.0	34.3	13.4	15.7	21.5	31.2
7)	$Red\ Clover_w$	35.0	34.3	14.2	15.5	22.8	33.1
8)	$Carrot_s$	30.0	28.5	20.0	24.4	6.1	18.7
9)	$Dandelion_w$	35.0	34.0	13.8	15.0	53.0	91.3
10)	$Carrot_w$	35.0	32.2	14.4	17.3	81.0	139.5
11)	$Ginseng_w$	35.0	34.1	10.0	11.3	120.0	206.7

c, s and w stands for chopped, sliced and whole, aerial and root crops.

In the current study heat pump dryer proved to be energy efficient and productive. This was concluded based on the fact that the heat pump dryer took 5 days and 190 kWh of energy to reduce the average moisture content of ginseng roots below 10%, while commercial dryers currently in use take about 14 days and 244 kWh of energy (van Dalfsen et al., 1992). This led to the conclusion that heat pump dryers are 22% more energy efficient and can reduce the drying time by 65% compared to conventional dryers incorporating electric coil heaters. The energy consumed by a blower/fan is ignored in the above comparison. The reason for such a big difference in efficiency and drying time is due to the ability of heat pump system to dehumidify (recover energy) the air before heating and re-circulating it through the material. In fact for low temperature (30°C to 45°C), conventional heated air drying may not be able to be used at all if the outdoor temperature and relative humidity are higher. Ginseng roots are usually grown in coastal regions where the atmospheric humidity level is high. Therefore, dehumidification of process air before entering the condenser coil and drying chamber can make a significant difference.

The drying of whole and chopped, alfalfa and red clover in Table 10 shows that the energy consumption during drying increased almost by three fold with the decrease in surface area to mass ratio of whole aerial crops compared to chopped material. Therefore, it is advised to chop the aerial crops in order to expedite the drying process and conserve energy.

The drying results of catnip, wormwood, red clover, portulaca, whole and sliced roots of carrots and dandelion were not compared, as there was no relevant published experimental data available to the knowledge of the authors.

5. TASK C – Computer Based Heat Pump Dryer Model

The modeling strategy adopted in this project involves the development of separate simulation models for the heat pump and dryer, and combine them using the laws of conservation of energy.

5.1 Dryer model – Thin layer

During drying, agricultural material undergoes a process of simultaneous heat and mass transfer. Heat is required to evaporate the moisture, which is removed from the drying product surface by the external drying medium, usually, air. Most materials, when dried under constant external conditions, exhibit a constant rate of moisture loss, followed by a falling rate drying period. The constant rate period is not a characteristic of normal agricultural drying. It is reasonably well established that most of the drying of agricultural products takes place in the falling rate period. Several models have been proposed for describing the transfer of moisture in capillary porous products during the falling rate period. The most accepted equations were developed by Luikov (1980). A simplification of the solution to the equations developed by Luikov (1980) was done by Crank (1979). This simplified solution is frequently used to describe the thin layer drying of agricultural material (Bala, 1997). The basic equation is given by

$$MR = \frac{M - M_e}{M_o - M_e} = \exp(-kt) \tag{9}$$

where,

t = time, min,
k = drying rate constant, min^{-1},
MR = moisture Ratio (fraction),
M = moisture content at time t,
M_e = equilibrium moisture content, and
M_o = initial moisture content.

Figure 20 shows two elemental volumes (dxdy) taken from conveyors C1 and C2 (Figure 4), each of length, L, and at an arbitrary location, but exactly in line with the cross-flow air stream.

It was assumed that the dryer takes a total time, t_t, to dry the material. This time can be divided into an equal number of small intervals, N, in such a way that the change in material property can be assumed to be negligible in that interval. The material will take equal time to pass through conveyors C1 and C2. An iterative procedure is used to find the temperature of air, T_a, the temperature of agricultural material, T_g, the humidity ratio, W, and the moisture content of material, M, at different time intervals. To find T_a, T_g, W and M, drying rate, mass balance, energy balance and heat transfer rate equations are required.

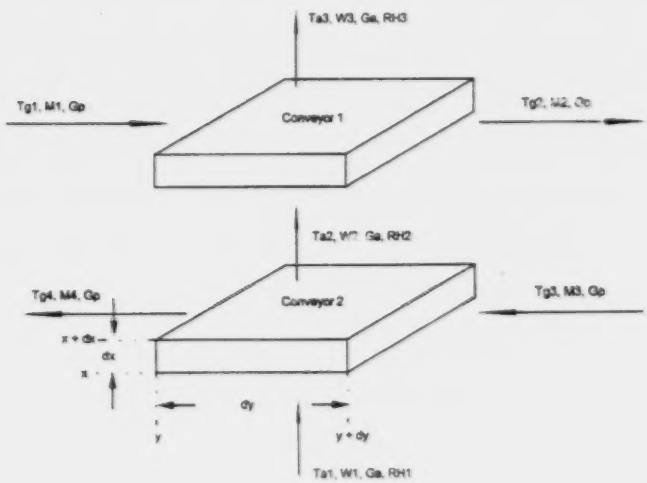

Figure 20. Psychrometric and material conditions at the two elemental volumes on conveyors one and two

5.1.1 Drying rate equation

Prediction of drying rate is important in the design of drying systems. Drying rate can be determined directly from the thin layer drying equation. This equation is used to find the moisture content of material at any time t $(t \le t_t)$ while drying. The rate of change in

moisture content is equal to an appropriate thin layer drying equation, which can be expressed as

$$\frac{\partial M}{\partial t} = -k(M - M_e) \tag{10}$$

Moisture content and time are integrated from their initial values of M_o and t_o to the final values of M and t. M_o is the initial moisture content of the material at time t_o, and M is moisture content of material at any time, t, on the drying bed. After integration we get

$$M = M_e + (M_o - M_e) \cdot a \cdot e^{-kt} \tag{11}$$

where,

$$a = e^{kt_o}$$

The drying constant, k, and equilibrium moisture content, M_e, varies for different agricultural materials. Usually they are determined experimentally. The following equations for the drying constant and equilibrium moisture content are for alfalfa, taken from Sokhansanj et al. (1996),

$$M_e = \left[\frac{1}{cT}\ln\left(\frac{1}{1-RH}\right)\right]^{\frac{1}{m}} \tag{12}$$

where,

T = temperature, °K, and

c and m are material constants which for alfalfa are 0.0000851 and 1.013, respectively.

The drying constant is not actually a constant but depends on the air temperature,

$$k = 0.2865\exp(0.179T_a) \tag{13}$$

where,

T_a = air temperature, °F, and

k is expressed in h^{-1}

From equation (11), moisture content of the material to be dried can be found at any time, t.

5.1.2 Mass balance equation

When a material undergoes drying, there exists a mass balance between the material and the process air. This implies that the change in moisture content of the air while passing through the material will be equal to the change in material moisture content given by

$$\frac{\partial W}{\partial x} = -\frac{G_p}{G_a}\frac{\partial M}{\partial y} \tag{14}$$

Humidity ratio, W, and thickness of bed in the x direction are integrated from their initial values of W_o and x_o to final values of W and x. In equation (14), the moisture content, M, at any point, y, along the drying bed can be determined using equation (11). After integration we get

$$W = W_o + bx \tag{15}$$

where,

$$b = -\frac{G_p}{G_a}\frac{\partial M}{\partial y}$$

x_o = 0 at all points on the drying bed, assuming no change in material properties in the x direction

Equation (15) can be used to calculate the change in humidity ratio as the air passes through the bed.

5.1.3 Energy balance equation

Energy balance exists in a dryer, when there are no unknown energy losses or air leaks to the surroundings. According to the energy balance equation, a change in enthalpy of air is equal to the heat transferred convectively to the material and that supplied to air in the evaporated moisture. The energy balance equation was rearranged and solved to get it in terms of the air temperature gradient across the drying bed thickness, x.

$$\frac{\partial T_a}{\partial x} = -\frac{\left(h_{cv} + G_a C_{pw}\left(\frac{\partial W}{\partial x}\right)\right)\left(T_a - T_g\right)}{G_a\left(C_{pa} + C_{pw}W\right)} \tag{16}$$

The temperature of the air, T_a, and thickness of the bed, x, are integrated from initial values of T_{ao} and x_o to final values of T_a and x. Change in humidity ratio of air, while passing across the bed in the y direction is obtained from equation (15). The final form of the equation will come out to be

$$T_a = T_g + e^{\frac{d}{e}x}\left(T_{ao} - T_g\right) \tag{17}$$

where,

$$d = h_{cv} + G_a C_{pw}\left(\frac{\partial W}{\partial x}\right),$$

$$e = G_a\left(C_{pa} + C_{pw}W\right),$$

x_o = 0 at all points on the drying bed,

C_{pw} = specific heat of water vapor, kJ/kg°K,

C_{pa} = specific heat of air, kJ/kg°K, and

h_{cv} = heat transfer coefficient, kJ/m^{3}min-°K.

The temperature of the air at the exit for the bed is calculated using equation (17).

5.1.4 Heat transfer rate equation

When the material undergoes drying, both sensible and latent heat transfer takes place between the material and process air. The heat transfer rate between the process air and material is equal to the sum of change in sensible heat of the material and net enthalpy change of air due to the moisture evaporation which can be expressed as temperature gradient in the y direction as

$$\frac{\partial T_g}{\partial y} = \left(\frac{h_{cv}\left(T_a - T_g\right) - \left(G_a\left(L_g + \left(C_{pw} - C_{pl}\right)T_g\right)\right)\left(\frac{\partial W}{\partial x}\right)}{-G_p\left(C_{pg} + MC_{pl}\right)}\right) \tag{18}$$

The temperature of the material, T_g, and distance along the bed, y, are integrated from their initial values of T_{go} and y_o. T_{go} is the temperature of material at distance, y_o, and T_g is temperature of material after traveling a distance, y, along the bed. The final value of material temperature, T_g, and its position, y, in the present iteration are the initial values T_{go} and y_o in the next step of the iteration process. Equation (18) is solved to obtain

$$T_g = \frac{1}{g}\left((f + gT_{go}) e^{\left(\frac{y-y_o}{h}\right)} - f \right) \tag{19}$$

where,

$$f = h_{cv} T_{ao} - G_a L_g \frac{\partial W}{\partial x},$$

$$g = \left(-h_{cv} + (C_{pw} - C_{pl}) G_a \frac{\partial W}{\partial x} \right),$$

$$h = -G_p (C_{pg} + MC_{pl}),$$

C_{pl} = specific heat of liquid, kJ/kg°K,

C_{pg} = specific heat of material, kJ/kg°K, and

L_g = latent heat of vaporization of moisture from material, kJ/kg.

Equation (19) can be used to find the variation in the material temperature while passing through the dryer.

5.2 Heat pump model

The basic purpose of a heat pump in a dryer is to supply hot air to the drying chamber at the desired temperature and to dehumidify the exhaust air coming from the drying chamber. To achieve the desired drying conditions, it is important that, the heat pump should be matched properly with the dryer.

The main purpose of developing the present heat pump model is providing information for predicting performance, which can be of assistance in the design of heat pump dryer systems for specialty crops. In this research, it is assumed that the heat pump will be subjected to

constant operating conditions associated with continuous drying. The spatial average and not the local conditions of heat pump were used to find the overall heat transfer coefficients at the condenser and evaporator coils.

It was decided to modify the actual refrigeration cycle, through some assumptions before modeling the heat pump system. Figure 21 represents an actual refrigeration cycle in which different pressure and energy losses of refrigerant in condenser and evaporator coils are depicted.

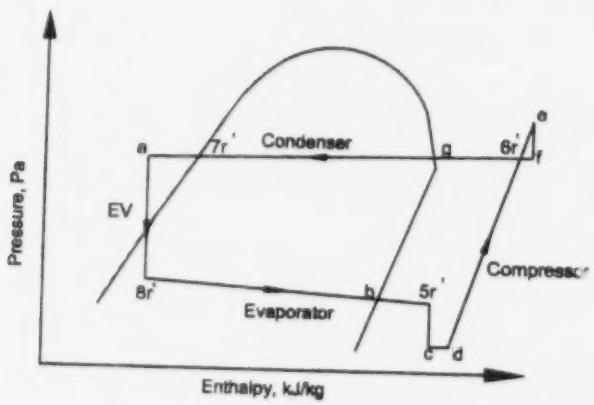

Figure 21. Actual heat pump cycle

Figure 21 was simplified to get an ideal refrigeration cycle (Figure 22).

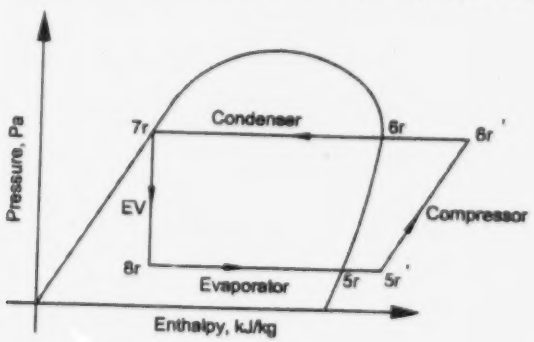

Figure 22. Ideal heat pump cycle

To get the ideal refrigeration cycle, the following assumptions were considered in actual cycle (Figure 21)

a) No suction line heating (b-5r')
b) No suction valve pressure drop (5r'-c)

c) No cylinder heating of vapor (c-d)

d) Iso-entropic compression (d-e)

e) No discharge valve pressure drop (e-f)

f) No discharge line heat loss (f-6r')

g) No pressure drop in condenser and evaporator coils (g-7r' and 8r'-b)

h) No liquid line heat loss or sub-cooling (7r'-a)

The energy transfer between the refrigerant and process air at the evaporator and condenser coil is given by the following equations

$$q_{evp} = U_{oe} A_{oe} (H - H_{sR}) \tag{20}$$

$$q_{cond} = U_{oc} A_{oc} \Delta T_{LMTDcond} \tag{21}$$

The energy transfer at the evaporator depends on the overall heat transfer coefficient, U_{oe}, surface area of the evaporator coil, A_{oe}, and the enthalpy difference of moist air calculated at the average air temperature, H and average refrigerant temperature, H_{sR}. It is important to note here that although U_{oe} is conventionally called overall heat transfer coefficient (Clements et al., 1993; Theerakulpisut, 1990; Threlkeld, 1970), its unit is different i.e. $kg/m^2/s$ instead of $W/m^2/K$.

Similarly, the energy transfer at the condenser depends on the overall heat transfer coefficient, U_{oc}, surface area of the condenser coil, A_{oc}, and the logarithmic mean temperature difference between the air and refrigerant, $\Delta T_{LMTDcond}$.

5.2.1 Overall heat transfer coefficient at condenser coil

The condenser is easier to model than the evaporator because of the absence of liquid at the outer surface of the condenser coil. The principal task of the condenser model in the heat pump dryer is to predict the energy transfer, the mass flow rate and temperature of the refrigerant at the condenser coil. For finding the above parameters, the overall heat transfer coefficient for the condenser, U_{oc}, must be known. It can be computed by using equation (22), which assumes negligible tube wall and fouling resistance. Equation (22) is taken from Jolly et al. (1990).

$$U_{oc} = \frac{1}{\frac{A_c}{A_{ti}h_i} + \frac{1-\phi_{eff}}{h_o\left(\frac{A_{to}}{A_f} + \phi_{eff}\right)} + \frac{1}{h_o}} \tag{22}$$

where,

h_i = inside (refrigerant) heat transfer coefficient, W/m^2-K,

h_o = outside (air) heat transfer coefficient, W/m^2-K,

A_c = total Condenser outside area, m^2,

A_{ti} = inside condenser tube area, m^2,

A_{to} = outside condenser tube area, m^2,

A_f = total condenser fin area, m^2, and

ϕ_{eff} = fin efficiency.

5.2.2 Overall heat transfer coefficient at evaporator coil

The important function of the evaporator is to remove moisture from the system by dehumidification of the exhaust air from the dryer. Sensible and latent heat are also recovered which would have otherwise lost to the atmosphere. With dehumidification, the airside surface can be wetted with liquid or frost. Condensation of moisture at the evaporator coil makes it difficult to model. Water-vapor transfer does not depend on temperature difference alone, instead it depends more on the difference between moist air enthalpy, H and enthalpy of moist air calculated at refrigerant temperature, H_{sR}. The task of the evaporator model is to predict the total energy transfer from the refrigerant to the process air and the temperature and mass flow rate of refrigerant. It is assumed that dehumidification occurs only on the two-phase section of the evaporator coil. The overall heat transfer coefficient at evaporator is required.

$$q_{evp} = U_{oe}A_e\left(H - H_{sR}\right) \tag{23}$$

where,

U_{oe} = overall heat transfer coefficient for the wet surface based on enthalpy difference, kg/m^2/s,

H = enthalpy of air, kJ/kg, and

H_{sr} = enthalpy of saturated air evaluated at refrigerant temperature, kJ/kg.

U_{oe} can be computed by using equation (24), which assumes negligible tube wall and fouling resistance. This equation is taken from Jolly et al. (1990), which is the modified form of equation given by Threlkeld (1970) and Turaga et al. (1988)

$$U_{o,e} = \frac{1}{\frac{b_R A_{oe}}{A_{pie}} + \frac{b_{wm}\left(1-\phi_{eff}\right)}{h_{ow}\left(\frac{A_{p,o}}{A_F}+\phi_{eff}\right)} + \frac{b_{wm}}{h_{ow}}} \tag{24}$$

where,

A_{oe} = total evaporator area, m^2,

A_{pie} = inside evaporator pipe area, m^2,

A_{po} = outside pipe evaporator area, m^2,

A_F = total evaporator fin area, m^2, and

h_{ow} = outside wet convective heat transfer coefficient, W/m^2-K.

In order to calculate U_{oe} from equation (24), values of the mean water film surface temperature, t_{wm}, and the pipe temperature, t_p, are assumed. These assumptions allow initial approximations to be made for b_{wm} and b_R respectively. After calculation of U_{oe}, the assumptions can be checked.

In the ideal cycle (Figure 22) 5r-5r' and 6r'-6r are superheating and de-superheating sections for the refrigerant fluid. The evaporator coil is divided into two sections, superheat and two-phase. In the superheat section, a superheat temperature increase of 5°C has been assumed, to avoid liquid refrigerant entering the compressor. The refrigerant is then compressed iso-entropically before entering the condenser. Using the effectiveness NTU (Number of Transfer Units) method on the condenser and evaporator coils, it was found that the fractions

of superheating and de-superheating areas were very small (0.001% of total coil area). Hence, the amount of heat transfer through these sections was neglected. The final refrigerant cycle left was 5r-6r-7r-8r (Figure 23) with only two-phase sections of refrigerant at condenser and evaporator coils.

Figure 23 shows the modeled pressure – enthalpy diagram for refrigerant circulating inside the heat pump.

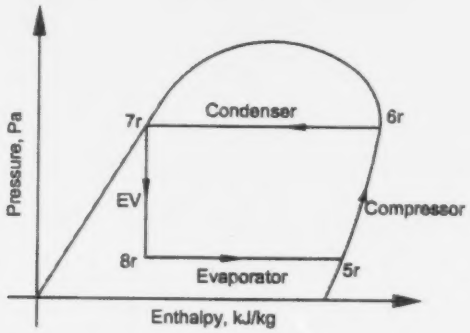

Figure 23. Modeled pressure-enthalpy diagram for refrigeration cycle

5.2.3 Compressor and Expansion Valve Model

The compressor is by far the most complex component in the heat pump. The major difficulties in mathematical modeling of compressors arise from the lack of understanding of basic knowledge of fluid flow, heat transfer and thermodynamics of the processes occurring within the compressor. According to Theerakulpisut (1990) and as discussed by Qvale et al. (1972), a very complex compressor model accounting for various processes within the compressor could be embedded in the heat pump simulation model. Unfortunately the size and complexity of such a compressor model would tend to overshadow the rest of the heat pump simulation. To simplify the calculations; constant volumetric efficiency and isentropic compression of the refrigerant must be assumed. A more detailed model could be used, as described by Fischer and Rice (1983), although this would require detailed manufacturer performance data, which can be difficult to obtain.

In the expansion valve model, a capillary tube will be used. It controls the amount of superheat at the evaporator outlet. The expansion process is assumed to be isenthalpic. If the manufacturer performance data are available, the refrigerant mass flow rate through the capillary tube can be calculated. Otherwise, the capacity of the expansion valve is assumed large enough so that the refrigerant mass flow rate passing through the capillary tube is same as that through the compressor.

5.3 Model Validation

As the first step in model verification, it was decided to perform a few preliminary experiments using a small cabinet dryer in a stationary tray or batch process. In continuous drying, psychrometric properties usually change very little over time. Hence, the verification of a computer model will become difficult, as there will be only a single set of data from each experiment. To get a better idea of model accuracy (uncertainty in prediction) it is important to have at least 10 sets of data from each experiment. This is only possible when stationary tray drying experiments are performed. In stationary tray drying the psychrometric properties of air will be transient and the data sets obtained will help in establishing the reliability of the simulation model. The cabinet dryer used in this study could also be a more economically viable heat pump dryer for smaller sized specialty crop operations. Figure 24 is a basic schematic diagram of the cabinet dryer used in this study.

Comprehensive computer models for a heat pump and a dryer were developed using the fundamentals of thermodynamics. The dryer and heat pump models were combined to get a single heat pump dryer system. The exit conditions of air from the dryer were taken as inlet conditions to the heat pump and the exit condition of air from the heat pump were taken as inlet conditions to the dryer.

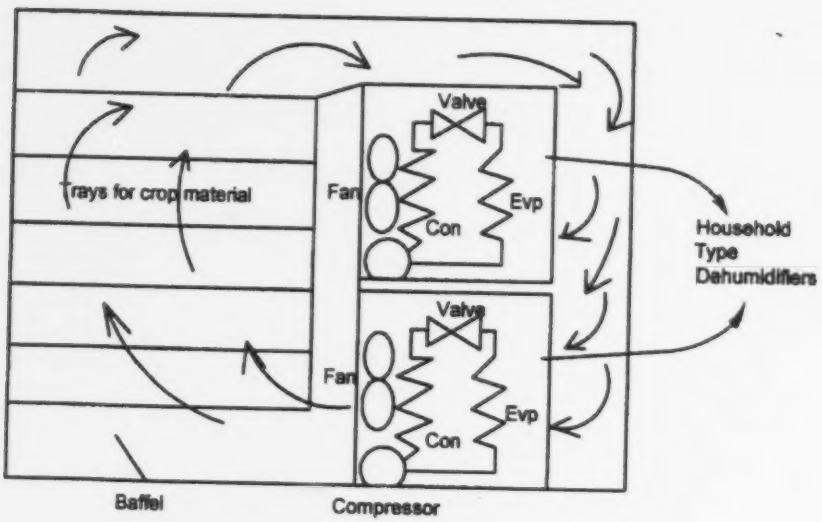

Figure 24. Basic schematic diagram of the cabinet heat pump dryer system

It is very important to validate the accuracy of simulation results with respect to experimental results. For this purpose the psychrometric conditions obtained from the cabinet and continuous bed drying experiments were used.

5.3.1 Validation of Simulation Model Using Cabinet Dryer Results

Alfalfa was the material used in experiments for validating the simulation model of the cabinet dryer system. The reason for using alfalfa instead of specialty crops like ginseng, herbs, echinacea, feverfew, etc., was that the material and knowledge about its drying properties were readily available. Also the structure of alfalfa leaves and stems is similar to that of many herbs and other specialty crops.

Figure 25 depicts the variation in temperature measured at the condenser and evaporator coils. An error and/or difference between the predicted and measured temperatures of ±4°C

at the condenser coil and ±5°C at the evaporator coil were observed. All the curves generally showed good agreement in the temperature variation pattern.

It is of paramount importance to do uncertainty analysis of the experimental temperatures obtained, in order to verify whether the simulation results are within the permissible error limit or not. The uncertainty analysis results predicted an error limit of ±5°C at the condenser and ±6°C at the evaporator coils (Adapa, 2001). The differences observed in the temperatures obtained from simulation and experimental results (Figure 25) are within these uncertainty limits.

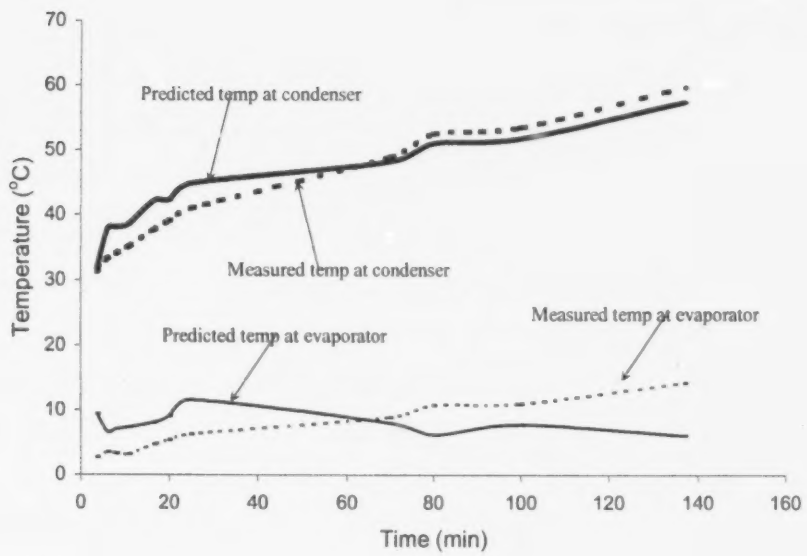

Figure 25. Comparison of measured and simulation temperatures of refrigerant at condenser and evaporator coils (during batch drying)

Figure 26 represents the change in moisture extraction rate (MER) from the material over time. The moisture loss through the inlet and outlet ports was taken into consideration in calculating the predicted results. The MER increased initially with an increase in moisture condensation rate. The moisture condensation rate was high because of high relative humidity at the dryer exit. Also, as the drying continued, the relative humidity of process air decreased thus reducing the MER. A good agreement between general shape of the curves

for the simulation and experimental results was observed. At any given time interval, the MER obtained experimentally was approximately 19% lower than obtained by simulation. This was expected. In weighing the material, the drying chamber door was opened for couple of minutes while removing and replacing all the trays. Thus was not possible to accurately determine the amount of process air leaked to ambient. Another problem was that the droplets of condensed moisture at the evaporator took some time to form a stream and flow through the tubes to the collection container. Thus the shape of the curve is the most important indicator of model accuracy and it agrees quite well with the experimental results.

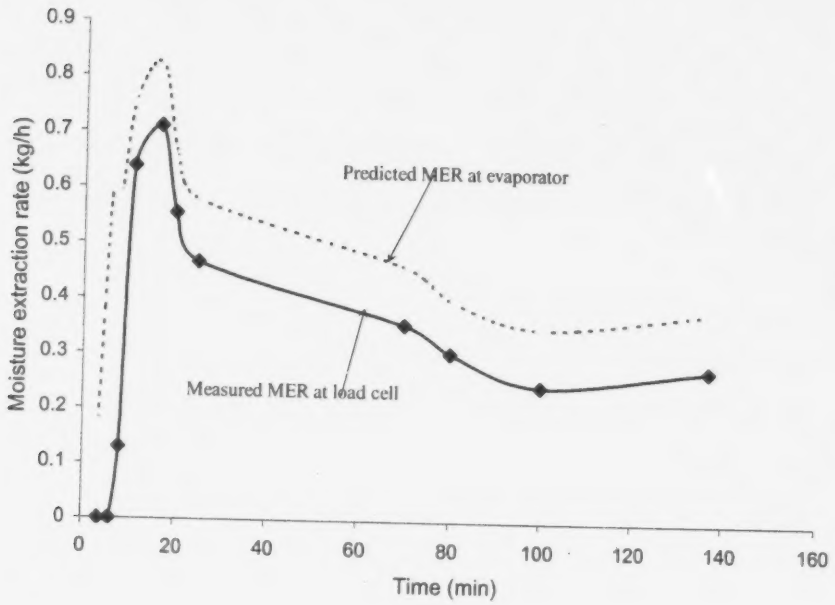

Figure 26. Moisture extraction rate for experimental and simulation results over material drying time (batch process only)

5.3.2 Validation of Continuous Bed Prototype Heat Pump Simulation Model

The geometric parameters and fluid and heat flow equations were modified for the cabinet dryer to fit the prototype (full-scale) heat pump dryer system. In this section, predicted results for the alfalfa are presented and discussed.

Table 4 (material drying properties) provides the experimental data for alfalfa drying. The alfalfa was dried at a temperature of 30°C with an initial moisture content of 67%, material flow rate of 2.9 kg/h in a material bed thickness of 0.03 m. The final moisture content of alfalfa after 3.3 h of drying was 10.4%. Using the simulation model for the prototype heat pump dryer, the results for alfalfa drying were predicted. It was determined that at similar drying conditions (same as that used for experimental purpose), the predicted final moisture content of alfalfa is 9.4%. This result agrees quite well with the experimental result. The predicted air humidity ratio at dryer exit was in exact agreement with the measured value (0.0055 kg/kg dry air) and the measured and predicted dryer exit air temperatures differed by about 4°C.

It is interesting to note that the drying rate equation for alfalfa in the model would work equally well for wormwood and red clover. Catnip would require some minor modifications to the equation while substantial modifications would be required to get good agreement for portulaca and root crops.

Figure 27 shows the variation in moisture content of alfalfa at the dryer exit as its mass flow rate through the drying chamber is increased. The temperature and relative humidity of air at the dryer inlet are varied, keeping the air humidity ratio constant. Simulation results are obtained at three different temperatures of 50°C, 40°C and 30°C with respective relative humidity values of 8%, 12% and 22%. The dryer inlet air humidity ratio was kept constant at 5.5 g/kg of dry air. All three curves show the same general behavior. The lowest moisture content is obtained for an inlet air temperature of 50°C because, with the increase in inlet air temperature, vapor pressure inside alfalfa increases and hence, it can diffused moisture more readily into the process air. However, there was not a significant difference in the amount of moisture removed between the three air temperatures studied.

In Figure 27, there is a sharp drop in moisture content of alfalfa chops at the dryer exit for mass flow rates below about 15 kg/h. Therefore, for the prototype drying system, the amount of moisture removed from alfalfa will be less if the mass flow rate of alfalfa chops is

above 15 kg/h under the given psychrometric conditions. This likely occurs because the initial moisture removed from alfalfa is at its surface and can be readily removed. It takes extra energy and time to remove the moisture present at the core of the material. Therefore, at mass flow rates below 15 kg/h, alfalfa gets enough time and exposure to the process air to diffuse moisture from the core to the surface.

The safe limit of 10% mc at dryer exit was obtained when the mass flow rate of alfalfa was only 2.0 - 4.5 kg/h. The mass flow rate for alfalfa at a drying air temperature of 30°C was 2.8 – 2.9 kg/h which agrees very well with values in Table 5.

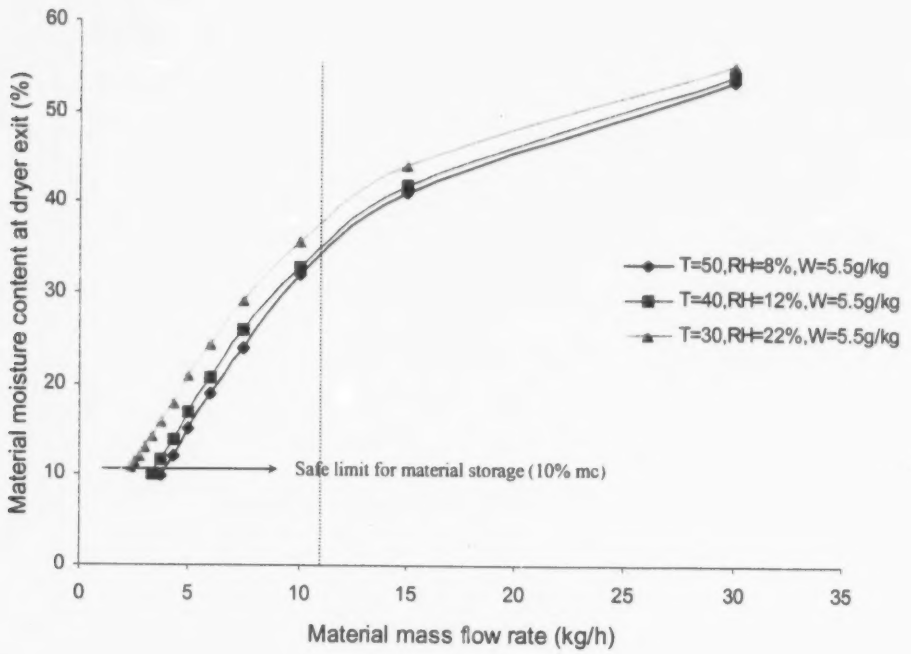

Figure 27. Predicted affect of alfalfa mass flow rate on its moisture content at the dryer exit

A similar model was also developed to determine proper size of a drying chamber, airflow rate and psychrometric properties of air to help in the appropriate selection of a heat pump. User's manual and programmer guide for both heat pump dryer and drying chamber design simulation models are provided in appendix C.

6. Conclusions

The results indicated that the required experimental low temperature drying conditions for specialty crops were achieved and also that all the objectives of the present investigation were accomplished. Heat pumps have their own advantages over other drying techniques. They provide energy savings (recovering latent and sensible heat at the evaporator) and environmental benefits through reduced air pollution. However, better quality of dried product is the major reason for using heat pump dryers. The current research led to the following general conclusions:

1) The heat pump dryers are 22% more energy efficient and can reduce the drying time by 65% compared to conventional dryers incorporating electric coil heaters.
2) Low temperatures (30-45°C) for safe drying of heat sensitive crops were achieved experimentally, which will help in maintaining better quality and conserve all the nutrients of the product.
3) The drying rate for most of the chopped leaf and stem material was similar, except portulaca, which caked while drying and took longer period to dry. On the other hand, drying rate of whole roots (carrots, dandelion and ginseng) was substantially longer. The difference was primarily due to their physical structure.
4) Chopped aerial crops dried almost seven times faster than whole aerial parts. Therefore, it is advised to chop the aerial crops in order to expedite the drying process.
5) No discoloration of aerial crops was observed during and after drying when inspected with the naked eye.
6) The simulation and experimental results for a prototype heat pump dryer agreed quite well with each other. Which establishes the reliability of the developed software for determining the drying properties of a material and heat pump system.
7) The cabinet dryer was shown to be capable of SMER of between 0.5 and 1.02 kg/kWh. This agrees quite well with most of previous work (Hodgett, 1976; Baines, 1986; Prasertsan and Saen-Saby, 1998; Achariyaviriya et al., 2000). The condenser and evaporator coils of the household type dehumidifiers used in this investigation were not very effective in reducing the process air temperature close to the coil temperatures. Commercial quality heat pump systems would be much more effective.

8) The cabinet dryer was about 50% more efficient in recovering latent heat from the dryer exhaust air compared to the conventional dryers, even with the ineffective condenser and evaporator coils in the cabinet dryer.

9) Continuous or moving tray drying is potentially a better option than stationary tray or batch drying because high process air humidity ratios at the entrance of evaporator and, constant MER and SMER values can be maintained.

It may be worthwhile to investigate developing a hybrid drying system. In a hybrid drying system, a conventional low temperature heat pump dryer could be combined with other means of high temperature drying techniques such as, microwave drying, electric heater drying, fluidized bed drying, etc. Hybrid drying can be of importance, because of the inherent transport properties of moisture within the material particles, it takes a much longer time to remove the last 20-30% of moisture entrapped within the material than it does to remove the initial 70-80% of moisture. Therefore, high temperature drying techniques coupled with low temperature drying can be of importance in removing the last 20-30% of moisture much faster from the material than the low temperature drying alone, provided this could be done without a detrimental loss of product quality.

References

1. Achariyaviriya, S., Sopanronnarit, S. and Terdyothin, A. 2000. Mathematical model development and simulation of heat pump fruit dryer, Drying Technology, 18(1&2), pp. 479-591.

2. Adapa, P.K. 2001. Performance Study of a Heat Pump Assisted Dryer System for Specialty Crops, M.Sc. Thesis, University of Saskatchewan, Saskatoon, SK, Canada.

3. ASAE Standards. 2000. ASAE S358. Determination of Forage Moisture Content. ASAE Standards, St. Joseph, MI: ASAE.

4. ASHRAE Fundamentals. 1997. Chapter 6: Psychrometrics, Fundamentals Handbook, ASHRAE.

5. Bala, B.K. 1997. Drying and storage of cereal grains, Oxford and IBH Publishing Co. PVT. LTD., New Delhi, pp. 166-170

6. Baines, P.G. 1986. A comparative analysis of heat pump dryers, Ph.D. Thesis, University of Otago, New Zealand.

7. Clements, S., Jolly, P., and Jia, X. 1993 Experimental verification of a heat pump assisted continuous dryer simulation model, International Journal of Energy Research, Vol. 17, pp. 19-28.

8. Crank, J. 1979. The Mathematics of diffusion, Oxford University Press, Oxford.

9. Filho, O.A., and Strommen, I. 1996. The application of heat pump in drying of Boimaterials, Drying Technology, Vol. 14(9), pp. 2061-2090.

10. Fischer, S.K., and Rice, C.K. 1983. A steady state computer design model for air-to-air heat pumps, Oak Ridge National Laboratory, USA.

11. Green, R.H., and Roberts, L. 1996. The effect of air-coil design on the performance of heat pumps and air conditioners, ASHRAE Transactions, pp. 257-265.

12. Hodgett, D.L. 1976. Efficient drying using heat pump, Chemical Engineer, Vol. 311, July/August, pp. 510-512.

13. Jolly, P., Jia, X., and Clements, S. 1990. Heat pump assisted continuous drying, Part 1: Simulation model, International Journal of Energy Research, Vol. 14, 1990, pp. 757-770.

14. Luikov, A.V. 1980. Heat and mass transfer, Mir Publishers, Moscow.

15. McQuiston, F.C and Parker, J.D. 1998. Heating, Ventilating and Air Conditioning Analysis and Design- 4th Edition, John Wiley and Sons Inc., Canada, pp. 68-70.

16. Oliver, T.N. 1982. Process drying with a dehumidifying heat pump, International Symposium on the Industrial Application of Heat Pumps, Coventry, U.K. BHRA, MK43 OAJ, England, C2, pp. 73-88.

17. Prasertsan, S., and Saen-Saby, P. 1998. Heat pump drying of agricultural material, Drying Technology, Vol. 16(1 & 2), pp. 235-250.

18. Qvale, F.B., Soedel, W., Stevenson, H.J, Elson, J.P., and Coates, D.A. 1972. Problem areas in mathematical modeling and simulation of refrigerating compressors, ASHRAE Transactions, Vol. 72, Part 1, pp. 75-84.

19. Sokhansanj, S., Arinze, E.A., and Schoenau, G.J. 1996. Report on "Forage drying and storage", College of Engineering, University of Saskatchewan, Saskatoon, Canada, pp. 73-76.

20. Sokhansanj, S., Bailey, W.G. and van Dalfsen, K.B. 1999. Drying of North American Ginseng, Drying Technology, 17(10), pp. 2293-2308.

21. Sosle, V.R., Raghavan, G.S.V. and Kittler, R. 2000. Low temperature drying process for heat sensitive agri-food products, ASAE Annual International Meeting, Midwest Express Center, Milwaukee, Wisconsin, paper no. 006025, July 9-12.

22. Strommen, I., and Kramer, K. 1994. New application of heat pumps in drying process, Drying Technology, Vol. 12, pp. 889-901.

23. Tai, K.W., Zylla, R., Abbas, S.P., Devotta, S., Watson, F.A., and Holland, F.A. 1982. The potential for heat pumps in drying and dehumidification systems - I: Theoretical Considerations, Energy Research, Vol. 6, pp. 305-322.

24. Tai, K.W., Zylla, R., Diggory, P.J., Devotta, S., Watson, F.A., and Holland, F.A. 1982. The potential for heat pumps in drying and dehumidification systems - II: An Experimental Assessment of the Heat Pump Characteristics of a Heat Pump Dehumidification System Using R114, Energy Research, Vol. 6, pp. 323-331.

25. Tai, K.W., Devotta, S., Watson, F.A., and Holland, F.A. 1982. The potential for heat pumps in drying and dehumidification systems - III: An Experimental Assessment of the Dehumidification Characteristics of a Heat Pump Dehumidification System Using R114, Energy Research, Vol. 6, pp. 333-340.

26. Theerakulpisut, S. 1990. Modeling heat pump grain drying system, Ph.D. Thesis, University of Melbourne, Australia.

27. Threlkeld, J.L. 1970. Thermal environmental Engineering, Second Edition, Prentice Hall Inc.

28. Turaga, M., Lin, S. and Fazio, P.P. 1988. Correlation for heat transfer and pressure drop factors for direct expansion air cooling and dehumidifying coils, ASHRAE Transactions, Vol. 94, part 2, pp 616-629.

29. van Dalfsen, K.B, Bailey, W.G. and Guo, Y. 1992. Influence of airflow, loading rates and size sorting on the drying of American ginseng, International Journal of Drying Technology, pp. 1370 – 1378.

30. van Hooren, D.L. and Lester, H.R., Effect of conditioning and drying ginseng roots – interim report, 1990 year. Horticulture Research Institute of Ontario, Ontario Ministry of Agriculture and Food, Agriculture Canada Research Station, Delhi, Ontario, 1991, pp. 13.

Appendix A: Equations used for Modeling Refrigerant used in Cabinet Dryer

A.1 Condenser and Evaporator Coil Specifications

It is important to know the coil specifications for the calculation of the overall heat transfer coefficients at the evaporator, U_{oe} and the condenser, U_{oc} as given in Task C. The coil specifications given in this section are that of the household dehumidifier (manufactured by Canadian Tire Corporation Model-43-5404-8D1) used in the present experiments to verify the simulation model developed for the heat pump dryer system. The evaporator coil used in the household dehumidifier for the present experiments does not have any fins. While this is not likely a very efficient system, it was the only one available for experimental purposes.

Condenser coil Specifications:

Number of longitudinal rows	= 1
Number of transverse rows	= 10
Transverse distance between rows	= 0.0255 m
Tube material	= Brass
Tube wall thickness	= 0.00071 m
Tube radius, outside	= 0.005 m
Fin material	= Aluminum
Fin radius, outside	= 0.01275 m
Fin thickness	= 0.00013 m
Fin spacing	= 0.0019 m
Fin density	= 12 / inch or 473 fins / m
Length of each tube	= 0.27 m
Cross-sectional area of duct	= 0.27m x 0.255m
Total length of coil	= 2.7 m

Total air side condenser area (including fin area) = 0.632 m^2

Total inside condenser tube area = 0.073 m^2

Total outside condenser tube area = 0.08 m^2

Total fin area	= 0.552 m^2

Evaporator coil Specifications:

Number of longitudinal rows	= 2
Number of transverse rows	= 16
Transverse distance between rows	= 0.0169 m
Longitudinal distance between rows	= 0.0169 m
Tube material	= Aluminum
Tube wall thickness	= 0.00071 m
Length of each tube	= 0.24 m
Total length of coil	= 7.68 m
Total air side evaporator area	= 0.24 m^2
Total inside evaporator tube area	= 0.21 m^2
Total outside evaporator tube area	= 0.24 m^2

A.2 Thermophysical Properties of R-134A

Appendix A also presents the curve fitted data for R-134A (tetrafluoroethane), to find the thermodynamic and transport properties. The curves are fitted to data for saturated liquid and vapor lines. These lines are as shown below in Figure 28.

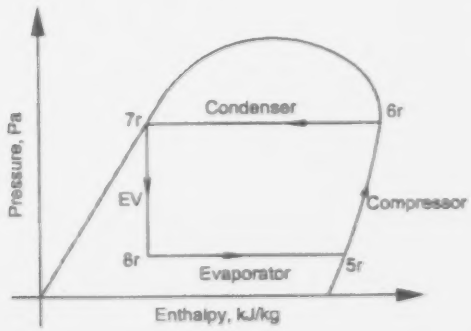

Figure 28. Pressure – enthalpy diagram for a refrigerant

ASHRAE (1997) data are curve fitted in order to simplify and speed up the calculation process, as it is very cumbersome to solve the non-linear differential equations to get the thermo-physical properties of a refrigerant. The error obtained between the curve-fitted data and the value given in ASHRAE (1997) is about ±1%. The following equations are for R-134A

A.2.1 Temperature (T, °C) - Enthalpy (H, J/kg)

A.2.1.1 Liquid saturation line

$$H = a_1 + a_2(T) + a_3(T)^2 + a_4(T)^3 + a_5(T)^4 + a_6(T)^5 \quad (25)$$

a_1 = 200002
a_2 = 1337
a_3 = 1.53
a_4 = 0.005944
a_5 = -0.00003226
a_6 = 0.000001202

A.2.1.2 Vapor saturation line

$$H = a_1 + a_2(T) + a_3(T)^2 + a_4(T)^3 + a_5(T)^4 + a_6(T)^5 \quad (26)$$

a_1 = 398685
a_2 = 583.4
a_3 = -1.102
a_4 = -0.008933
a_5 = 0.00004048
a_6 = -0.000001944

A.2.2 Temperature (T, °C) - Viscosity (Mu, Pa.s)

A.2.2.1 Liquid saturation line

$$Mu = a_1 + a_2(T) + a_3(T)^2 + a_4(T)^3 + a_5(T)^4 + a_6(T)^5 \quad (27)$$

a_1 = 0.0002873
a_2 = -0.000003573
a_3 = 2.956E-8
a_4 = -2.724E-10
a_5 = 1.842E-12
a_6 = -7.487E-15

A.2.2.2 Vapor saturation line

$$Mu = a_1 + a_2(T) + a_3(T)^2 + a_4(T)^3 + a_5(T)^4 + a_6(T)^5 \quad (28)$$

a_1 = 0.00001094
a_4 = 1.232E-12

a_2 = 4.637E-8
a_3 = 1.156E-11
a_5 = -5.159E-15
a_6 = 5.026E-16

A.2.3 Temperature (T, °C) - Thermal Conductivity (K, W/m-K)

A.2.3.1 Liquid saturation line

$$K = a_1 + a_2(T) + a_3(T)^2 + a_4(T)^3 + a_5(T)^4 + a_6(T)^5 \quad (29)$$

a_1 = 0.09339
a_2 = -0.0004596
a_3 = 4.952E-8
a_4 = -3.714E-9
a_5 = 7.619E-11
a_6 = -4.762E-13

A.2.3.2 Vapor saturation line

$$K = a_1 + a_2(T) + a_3(T)^2 + a_4(T)^3 + a_5(T)^4 + a_6(T)^5 \quad (30)$$

a_1 = 0.01179
a_2 = 0.00008611
a_3 = 8.913E-8
a_4 = 3.858E-9
a_5 = 8.69E-12
a_6 = -3.571E-14

A.2.4 Temperature (T, °C) - Specific Heat (Cp, J/kg-K)

A.2.4.1 Liquid saturation line

$$Cp = a_1 + a_2(T) + a_3(T)^2 + a_4(T)^3 + a_5(T)^4 + a_6(T)^5 \quad (31)$$

a_1 = 1336
a_2 = 3.078
a_3 = 0.00711
a_4 = -0.0002756
a_5 = 1.732E-05
a_6 = -3.862E-08

A.2.4.2 Vapor saturation line

$$Cp = a_1 + a_2(T) + a_3(T)^2 + a_4(T)^3 + a_5(T)^4 + a_6(T)^5 \quad (32)$$

a_1 = 878.4
a_2 = 4.373
a_3 = 0.08492
a_4 = 0.000155
a_5 = -0.00009301
a_6 = 11.98E-07

A.2.5 Temperature (T, °C) - Latent Heat of Vaporization (i_{fg}, J/kg)

$$i_{fg} = a_1 + a_2(T) + a_3(T)^2 + a_4(T)^3 + a_5(T)^4 + a_6(T)^5 \quad (33)$$

a_1 = 198681
a_2 = -753.4
a_3 = -2.623
a_4 = -0.01557
a_5 = 0.00008694
a_6 = -0.000003236

A.2.6 Temperature (T, °C) – Density of Refrigerant (ROH, kg/m^3)

A.2.6.1 Liquid saturation line

$$ROH = a_1 + a_2(T) + a_3(T)^2 + a_4(T)^3 + a_5(T)^4 + a_6(T)^5 \quad (34)$$

a_1 = 1294
a_2 = -3.266
a_3 = -0.007834
a_4 = -0.00004183
a_5 = -1.675E-07
a_6 = -8.122E-09

A.2.6.2 Vapor saturation line

$$ROH = a_1 + a_2(T) + a_3(T)^2 + a_4(T)^3 + a_5(T)^4 + a_6(T)^5 \quad (35)$$

a_1 = 14.4
a_2 = 0.5035
a_3 = 0.007261
a_4 = 0.00004913
a_5 = -1.724E-07
a_6 = 1.084E-08

A.2.7 Temperature (T, °C) – Pressure (P, MPa)

$$P = a_1 + a_2(T) + a_3(T)^2 + a_4(T)^3 + a_5(T)^4 + a_6(T)^5 \quad (36)$$

a_1 = 0.2927
a_2 = 0.01061
a_3 = 0.0001482
a_4 = 9.139E-07
a_5 = 1.191E-09
a_6 = 8.189E-12
a_7 = -1.5858E-11

A.3 Fin Efficiency

The fin efficiency is a function of the fin geometry and the airside heat transfer coefficient. Green and Roberts (1996) evaluated the fin efficiency for circular fins. Most of the heat exchanger coils consist of a tube-plate-finned arrangement. Therefore, considering the plate

fins to consists of a series of rectangular fins, the results of Green and Roberts (1996) can be used by considering equivalent circular fins, where the equivalent fin diameter is

$$D_{eqv} = 2\left(\frac{X_L . X_T}{\pi}\right)^{\frac{1}{2}} \tag{37}$$

and the equivalent fin height is

$$Z_{eqv} = \frac{\left(D_{eqv} - D_o\right)}{2} \tag{38}$$

where,

D_o = tube outside diameter.

Their data were formulated into equations for fin efficiency as a function of the parameters X and R where

$$X = Z_{eqv}\left(\frac{2.h_a}{k_f . Y_f}\right)^{\frac{1}{2}} \tag{39}$$

and $$R = \frac{D_{eqv}}{D_o}. \tag{40}$$

The fin efficiency (ϕ) is then defined using the following expressions:

For R = 1.0,

$$\phi = 1.03552448 - 0.31837607X + 0.02589744X^2 - 0.00101X^3; \tag{41}$$

for R = 1.5,

$$\phi = 1.04188811 - 0.3713209X + 0.04282051X^2 - 0.000637X^3; \tag{42}$$

for R = 2.0,

$$\phi = 1.03552448 - 0.45592852X + 0.08051282X^2 - 0.005004X^3; \tag{43}$$

for R = 3.0,

$$\phi = 1.03881119 - 0.5195338X + 0.10275058X^2 - 0.0070863X^3; \quad (44)$$

for R = 4.0,

$$\phi = 1.03230769 - 0.5540948X + 0.117016X^2 - 0.0087024X^3; \quad (45)$$

where,

D_{eqv} = equivalent fin diameter, m,

X_T = transverse distance between coil rows, m,

X_L = longitudinal distance between coil rows, m,

Z_{eqv} = equivalent fin height, m,

D_o = coil outside diameter, m,

k_f = thermal conductivity of fin,

Y_f = fin thickness, m, and

h_a = heat transfer coefficient, W/m^{2o}K.

Appendix B: Equations used for Modeling Refrigerant used in Prototype Heat Pump

B.1 Condenser and Evaporator Coil Specifications

The coil specifications are required for the calculation of overall heat transfer coefficients at the evaporator, U_{oe}, and condenser, U_{oc}, as given in TASK C. The coil specifications given in this section are that of the commercial dehumidifier manufactured by Blanchard-ness, model no. KOD-075-M4K and serial no. 2000020448.

Condenser coil Specifications

Number of longitudinal rows, Nr	= 6
Number of transverse rows, Nt	= 12
Longitudinal distance between rows, Pl	= 0.032 m
Transverse distance between rows, Pt	= 0.038 m
Tube material	= Copper
Tube wall thickness, Xp	= 0.00071 m
Tube radius, r1 (outside)	= 0.0063 m
Fin material	= Aluminum
Fin radius, r2 (outside)	= 0.019 m
Fin thickness, y	= 0.00013 m
Fin Spacing, Wf	= 0.0025 m
Fin density, fd	= 10 / inch or 394 fins / m
Length of each tube, Lt	= 0.61 m
Crossectional area of the air duct	= 2 ft x 2 ft or 0.3721 m^2
Total length of coil, L	= 43.92 m
Total air side condenser area (including fins area), A_{oc}	= 19.12 m^2
Total inside condenser tube area, A_{tic}	= 1.543 m^2
Total outside condenser tube area, A_{toc}	= 1.649 m^2
Total fin area, A_{fc}	= 17.47 m^2

Evaporator coil Specifications

Number of longitudinal rows, Nr	= 8
Number of transverse rows, Nt	= 15
Transverse distance between rows, Pt	= 0.038 m
Longitudinal distance between rows, Pl	= 0.038 m
Tube material	= Copper
Tube wall thickness	= 0.00071 m
Tube radius, r1 (outside)	= 0.0063 m
Fin material	= Aluminum
Fin radius, r2 (outside)	= 0.0214 m
Fin thickness, y	= 0.00013 m
Fin Spacing, Wf	= 0.0025 m
Fin density, fd	= 10 / inch or 394 fins / m
Length of each tube, Lt	= 0.61 m
Total length of coil, L	= 73.2 m
Crossectional area of the air duct	= 2 ft x 2 ft or 0.3721 m^2
Total air side evaporator area, A_{oe}	= 40.65 m^2
Total inside evaporator tube area, A_{pie}	= 2.57 m^2
Total outside evaporator tube area, A_{poe}	= 2.75 m^2
Total evaporator fin area, A_{fe}	= 37.89 m^2

B.2 Thermophysical Properties of R-404A

This section presents the curve fitted data for finding thermodynamic and transport properties of Refrigerant-404A. The curves are fitted to data for saturated liquid and vapor lines. These lines are as shown below in Figure 29.

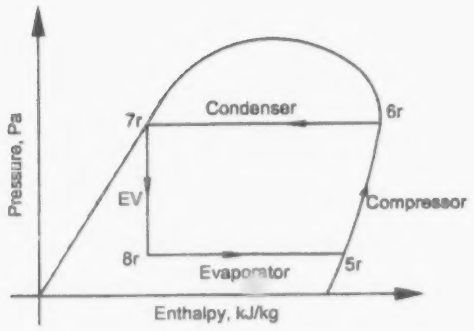

Figure 29. Pressure – enthalpy diagram for a refrigerant

ASHRAE (1997) data are curve fitted in order to simplify and speed up the calculation process, as it is very cumbersome to solve the non-linear differential equations to get the thermo-physical properties of a refrigerant. The error obtained between the curve fitted data and the values given in ASHRAE (1997) is about $\pm 1\%$. The following equations are for R-404A

B.2.1 Temperature (T, °C) - Enthalpy (H, J/kg)

B.2.1.1 Liquid saturation line

$$H = a_1 + a_2(T) + a_3(T)^2 + a_4(T)^3 + a_5(T)^4 + a_6(T)^5 \tag{46}$$

$a_1 = 200867$
$a_2 = 1461$
$a_3 = -2.904$
$a_7 = -0.0000006053$
$a_4 = -0.104$
$a_5 = 0.003367$
$a_6 = 0.00003732$

B.2.1.2 Vapor saturation line

$$H = a_1 + a_2(T) + a_3(T)^2 + a_4(T)^3 + a_5(T)^4 + a_6(T)^5 \tag{47}$$

$a_1 = 364895$
$a_2 = 507.9$
$a_3 = -2.837$
$a_7 = -0.0000005$
$a_4 = -0.02401$
$a_5 = 0.00143$
$a_6 = -0.0000001563$

B.2.2 Temperature (T, °C) - Viscosity (Mu, Pa.s)

B.2.2.1 Liquid saturation line

$$Mu = a_1 + a_2(T) + a_3(T)^2 + a_4(T)^3 + a_5(T)^4 + a_6(T)^5 \quad (48)$$

a_1 = 0.0002873
a_2 = -0.000003573
a_3 = 2.956E-8
a_4 = -2.724E-10
a_5 = 1.842E-12
a_6 = -7.487E-15

B.2.2.2 Vapor saturation line

$$Mu = a_1 + a_2(T) + a_3(T)^2 + a_4(T)^3 + a_5(T)^4 + a_6(T)^5 \quad (49)$$

a_1 = 0.00001094
a_2 = 4.637E-8
a_3 = 1.156E-11
a_4 = 1.232E-12
a_5 = -5.159E-15
a_6 = 5.026E-16

B.2.3 Temperature (T, °C) - Thermal Conductivity (K, W/m-K)

B.2.3.1 Liquid saturation line

$$K = a_1 + a_2(T) + a_3(T)^2 + a_4(T)^3 + a_5(T)^4 + a_6(T)^5 \quad (50)$$

a_1 = 0.09339
a_2 = -0.0004596
a_3 = 4.952E-8
a_4 = -3.714E-9
a_5 = 7.619E-11
a_6 = -4.762E-13

B.2.3.2 Vapor saturation line

$$K = a_1 + a_2(T) + a_3(T)^2 + a_4(T)^3 + a_5(T)^4 + a_6(T)^5 \quad (51)$$

a_1 = 0.01179
a_2 = 0.00008611
a_3 = 8.913E-8
a_4 = 3.858E-9
a_5 = 8.69E-12
a_6 = -3.571E-14

B.2.4 Temperature (T, °C) - Specific Heat (Cp, J/kg-K)

B.2.4.1 Liquid saturation line

$$Cp = a_1 + a_2(T) + a_3(T)^2 + a_4(T)^3 + a_5(T)^4 + a_6(T)^5 \quad (52)$$

$a_1 = 1379$
$a_2 = 4.915$
$a_3 = 0.1123$
$a_4 = -0.0001953$
$a_5 = -0.00009864$
$a_6 = 0.0000004453$
$a_7 = 0.0000000344$

B.2.4.2 Vapor saturation line

$$Cp = a_1 + a_2(T) + a_3(T)^2 + a_4(T)^3 + a_5(T)^4 + a_6(T)^5 \quad (53)$$

$a_1 = 984.2$
$a_2 = 6.766$
$a_3 = 0.1575$
$a_4 = -0.000224$
$a_5 = -0.0001474$
$a_6 = 0.0000006198$
$a_7 = 0.00000005141$

B.2.5 Temperature (T, °C) - Latent Heat of Vaporization (i_{fg}, J/kg)

$$i_{fg} = a_1 + a_2(T) + a_3(T)^2 + a_4(T)^3 + a_5(T)^4 + a_6(T)^5 \quad (54)$$

$a_1 = 164028$
$a_2 = -953.1$
$a_3 = 0.06661$
$a_4 = 0.07997$
$a_5 = -0.001937$
$a_6 = -0.00003747$
$a_7 = 0.0000001052$

B.2.6 Temperature (T, °C) – Density of Refrigerant (ROH, kg/m^3)

B.2.6.1 Liquid saturation line

$$ROH = a_1 + a_2(T) + a_3(T)^2 + a_4(T)^3 + a_5(T)^4 + a_6(T)^5 \quad (55)$$

$a_1 = 1149$
$a_2 = -4.039$
$a_3 = -0.001111$
$a_4 = 0.0002518$
$a_5 = -0.00006991$
$a_6 = -0.0000001268$
$a_7 = 6.619E-10$

B.2.6.2 Vapor saturation line

$$ROH = a_1 + a_2(T) + a_3(T)^2 + a_4(T)^3 + a_5(T)^4 + a_6(T)^5 \quad (56)$$

a_1 = 31.55
a_2 = 1.057
a_3 = 0.01356
a_4 = -0.00004312
a_5 = -3.002E-06
a_6 = 6.095E-08
a_7 = 1.548E-09

B.2.7 Temperature (T, °C) – Pressure (P, MPa)

$$P = a_1 + a_2(T) + a_3(T)^2 + a_4(T)^3 + a_5(T)^4 + a_6(T)^5 \quad (57)$$

a_1 = 0.6311
a_2 = 0.02064
a_3 = 0.0001319
a_4 = -0.000001458
a_5 = 7.63E-08
a_6 = 8.333E-10
a_7 = -1.5858E-11

Appendix C: Computer Simulation Model – Users Guide

C.1 Combined Heat Pump Dryer System

****

Program documentation and instructions for using combined heat pump counter cross-flow continuous bed dryer simulation model.

****

Programmer: Phani K. Adapa

Date: January 16, 2003

Organization: University of Saskatchewan

Version 1.0

****

1. User's Manual

The present combined heat pump dryer simulation model was obtained upon merging a heat pump and a dryer model. These models were prepared separately and later unified using the laws of heat and mass transfer. The heat pump dryer model has the ability to predict the average air and material temperature, average humidity ratio of air and average moisture content of the material at the dryer exit. It also predicts the refrigerant temperature at the evaporator and condenser coils along with refrigerant mass flow rate. The following are the instructions that a user may like to follow to get better results.

****How to run or use the program****

1) If possible use Visual FORTRAN
2) Open the file by double clicking on the program
3) Click the compile button on the screen to compile the program
4) Click command run to execute the program. A DOS window will open , prompting you to enter certain information
5) Enter the initial moisture content of material Mo, decimal
6) Enter the initial air temperature before entering the dryer TAO, degree Celsius
7) Enter relative humidity of air at the dryer inlet, decimal
8) Total time that may be required by the material to pass through the dryer, minutes (enter only even numbers)
9) Total length of dryer bed, m

10) Humidity ratio of air at the dryer entrance HO, kg/kg

11) Material layer thickness on conveyors X, m

12) Air mass flow rate GA, kg/min-m^2

13) Total mass of material to be dried MMF, kg

14) Specific heat of air CPA, kJ/kg-K

15) Specific heat of water vapor CPW, kJ/kg-K

16) Material temperature at the dryer entrance TGO, degree Celsius

17) Latent heat of vaporization of free water LW, kJ/kg

18) Specific heat of material CPG, kJ/kg-K

19) Specific heat of liquid CPL, kJ/kg-K

20) Air flow rate in the drying chamber ma, kg/s

21) Air temperature at evaporator exit T4, degree Celsius

22) Air temperature at condenser exit t1, degree Celsius

23) First predicted value of refrigerant temperature at the evaporator TPE, degree Celsius

24) First predicted value of refrigerant temperature at the condenser TPC, degree Celsius

2. Programmer's Guide

a) Statement of Purpose

To understand and predict the drying process of specialtv crops, it is important to develop a simulation model based on the existing thin layer drying equations and fundamentals of heat and mass transfer taking place at the evaporator and condenser coils of a heat pump system. This model will also help in designing an appropriate heat pump dryer system based on the quantity and type of material to be dried.

The heat pump dryer simulation model is obtained by combining separately developed heat pump and dryer models using the laws of conservation of heat and mass transfer. Due to the complexity in the problem definition and irregularity of the formulae, no sub-routines were used, instead a single program module was developed.

The first stage of the program (i.e. the dryer model) is used to determine the transient and average drying properties of the air and material inside the dryer. These properties includes the change in temperature and humidity ratio of air across the conveyor belts (air flowing from bottom to top) and change in temperature and moisture content of material while moving along the conveyor belts from inlet to the exit of the drying chamber.

The amount of time taken by the material to dry will depend on its drying rate and initial moisture content. Because of the structural difference chopped and whole aerials, and sliced and whole root crops will have significantly different drying rates. Based on the experiments conducted during this project, it was decided that the drying rate equation for alfalfa can be modified to be used for various crops (aerial and root). Refer to the table given below to get an idea of the constants that need to be multiplied to the drying rate equation of alfalfa to get approximate values for other materials.

Drying rate equation for alfalfa

$$k = 0.2865e^{\left(0.179\left(\frac{5}{9}(Tao-32)\right)\right)}\left(\frac{1}{60}\right)$$

where,

k = drying rate constant, 1/h and

Tao = air temperature at dryer inlet, °C.

Constants required to be multiplied to get drying rates for various aerial and root crops

Aerial Crops

Chopped	1 (Portulaca is an exception = 1/3)
Whole	1/7

Root Crops

Carrot and dandelion

Sliced	1/3
Whole	1/16

Ginseng

Whole	1/36

The second stage of the program (i.e. the heat pump model) is used to predict the moisture removal rate at the evaporator coil, mass flow rate of the refrigerant and average temperature of the refrigerant at the evaporator and condenser coils based on the psychrometric properties of air inside the dryer. Important parameters influencing the above four properties of a heat pump includes the inlet drying air temperature, air temperature at the exit of the evaporator coil, relative humidity of air at the dryer exit and mass flow rate of the air circulating inside the drying chamber. The air temperature at the exit of the evaporator coil was assumed constant at 5°C to avoid frost formation. The refrigerant used in the present simulation is R 404A. This program will not work if the temperature of the refrigerant exceeds its critical limit. For condenser and evaporator coil specifications, equations to find thermo-physical properties (enthalpy, viscosity, thermal conductivity, specific heat, latent heat of vaporization, density of refrigerant and pressure) of R 404A, refer to Appendix A and B.

b) Program Status and Limitations

The program created here works perfectly according to the thin layer drying equations and fundamentals of heat and mass transfer. During the program testing and gathering simulation results, no problem was encountered. The program code presented for the heat pump dryer is based on the assumption that the user is using refrigerant R 404A as the heat transfer medium. If the user is willing to use some other refrigerant then they may require replacing the existing thermo-physical property equations for R 404A with refrigerant specific equations. Also, depending upon the type of evaporator and condenser coils, the specifications regarding coil surface area may need to be replaced. Finally the program code will not work if the temperature of refrigerant exceeds its critical limit and will show a message stating that.

c) Test Cases/Data

The typical input values for any chopped aerial crops (having similar properties as alfalfa) are given below. Rest of the simulation results and their graphical representation is provided in the main body of the final project report.

Initial moisture content of material, Mo = 70%

Initial air temperature before entering the dryer, Tao =14°C

Total length of dryer bed, yy = 8 m

Thickness of layer of material, X = 0.025 m

Mass flowrate of air, Ga = 86 kg/min-m^2 or 1000 cfm

Specific heat of air, Cpa = 1.008 kJ/kg-K

Specific heat of water vapour, Cpw = 1.89 kJ/kg-K

Inlet temperature of material, Tgo = 14°C

Latent heat of vaporization of free water, Lw = 2501.64 kJ/kg

Specific heat of material, Cpg = 4.52 kJ/kg-K

Specific heat of liquid, Cpl = 4.186 kJ/kg-K

Inlet humidity ratio of process air to the dryer, kg/kg of dry air

Inlet relative humidity of process air to the dryer, %

Amount of material dried, kg

Total time period for which the material was inside the drying chamber, min

d) Program Output

Please refer to results provided in the main body of the report

3. Program Code

A soft copy of the simulation program is provided in a CD attached at the end of this manual.

C.2 Heat Pump Dryer Sizing

****

Program documentation and instructions to determine proper sizing of a drying chamber and air flow rate.

****

Programmer: Phani K. Adapa

Date: January 16, 2003

Organization: University of Saskatchewan

Version 1.0

****

1. User's Manual

For manufacturing any heat pump dryer system, it is essential to determine the drying chamber dimensions and psychrometric properties of circulating air in order to finalize heat pump specifications. The known conditions or information used for calculations are the type of material (aerial/root) to dry, material inlet and outlet moisture content, temperature of air at the dryer inlet and expected material mass flow rate. The information that the program will prompt the user to enter is:

****How to run or use the program****

1) Moisture content of material at dryer inlet Me, decimal
2) Moisture content of material at dryer exit Mfinal, decimal
3) Drying air temperature Tdry, degree Celsius
4) Mass flow rate of material or drying rate Mrate, kg/h
5) Air relative humidity at dryer inlet RHia, decimal

2. Programmer's Guide

Heat pump dryer specification program assumes that a user already has information about material inlet and outlet moisture content, equilibrium moisture content and dryer inlet air temperature. The unknowns that will be determined during this process are:

1) Equilibrium moisture content, Me

$$M_e = \left(\frac{1}{cT} \ln\left(\frac{1}{1 - RH_{ia}} \right) \right)^{\left(\frac{1}{m}\right)} \tag{58}$$

where,

RH_{ia} = air relative humidity at dryer inlet, decimal

c, m = material constants (values are 0.0000851 and 1.013, respectively)

T = temperature, K

2) Total time required for drying, t

$$t = -\left(\frac{2.6}{k}\right)\ln\left(\frac{M_f - M_i}{M_e - M_i}\right) \tag{59}$$

where,

k = drying constant, 1/h

M_f = final material moisture content, decimal

M_i = initial material moisture content, decimal

M_e = equilibrium moisture content of material, decimal

3) Total mass of material, M_t

$$M_t = M_m \times t \tag{60}$$

where,

M_m = mass flow rate of material, kg/h

t = total time required by the material to dry, h

4) Length of drying bed, l

$$M_t = \rho \times V = \rho \times l \times b \times d \tag{61}$$

where,

ρ = density of fresh material, kg/m^3 (for alfalfa at moisture content of 70% is 187 kg/m^3)

V = material volume, m^3

l = length of dryer bed, m

b = width of the dryer bed, m

d = thickness, m

The approximate length of the dryer bed can be obtained by using the equation developed during the experimentation. The equation is as follows:

$$l = -2.8 \ln\left(\frac{M_f}{0.6917}\right) \tag{62}$$

The value of length obtained from equation 62 can be used in equation 61 to determine the width of the conveyor bed.

5) Belt speed, s

$$s = \frac{l}{t} \tag{63}$$

where,

l = length, m

t = total time, h

6) Air flow rate, cfm

Finally air flow rate was calculated assuming a linear relationship between the air flow rate and surface area. This relationship was derived from the experimental results obtained during the tests performed on specialty crop material using prototype heat pump dryer system. According to this equation, air flow rate should increase with increase in surface area of the drying bed.

$$AFR = 505.1 \times l \times b \tag{64}$$

where,

AFR = air flow rate, cfm

l = length of the dryer bed, m

b = width of the dryer bed, m

3. Program Output

1) Initial moisture content of material, M_o
2) Final moisture content of material, Mfinal, decimal
3) Drying air temperature, Tdry, degree Celsius
4) Material mass flow rate, Mrate, kg/h
5) Inlet air relative humidity at dryer entrance, RHia, decimal
6) Equilibrium moisture content, Me, decimal

7) Time required to dry the material, t, h
8) Total mass of material on bed, Mt, kg
9) Length of drying bed, l, m
10) Thickness of the material bed, d, m
11) Width of the drying bed, b, m
12) Speed of conveyor bed during drying, s, m/h
13) Required air flow rate for drying, AFR, cm
14) Maximum air temperature at condenser exit, degree Celsius
15) Minimum air temperature at evaporator exit, degree Celsius

4. Program Code

A soft copy of the simulation program is provided in a CD attached at the end of this manual.

Indications for Further Development

The prototype continuous bed heat pump dryer developed is capable of drying 2-4.5 kg/h of aerial (leaf and stem) material and it's re-circulating nature made it 22% more energy efficient and reduced the drying time by 65% compared to conventional dryers. Even though the drying efficiencies increased, the drying of specialty crops (especially roots and whole plants) takes longer time. Investigation of a new approach, such as developing a hybrid drying system, is essential. In a hybrid drying system, a low temperature heat pump dryer will be combined with a microwave to enhance drying rate and in turn could further increase the dryer efficiency. A decrease in process (drying) time, sustained product quality and an increase in dryer efficiency can improve the profit margin and can lure more farmers to stay in the agricultural industry.

The limitation of relatively low-heat transfer rates in a heat pump dryer, particularly toward the falling rate period, can be overcome by taking advantage of volumetric heat generation during microwave heating. A microwave generates heat volumetrically within the material wetted with polar molecules such as water by the combined mechanisms of dipole rotation and ionic conduction. Such internal heat generation speeds up the drying process mainly because of unidirectional temperature and moisture concentration gradients, internal pressure build-up, and short time delay. Non-polar materials, such as fat or oil, and dry solids, which usually form a skeleton of the material being dried, do not react essentially to the electromagnetic field, therefore, they are not directly heated by microwave energy.

Most commercial materials to be dried have molecules, which are electrically symmetrical. Therefore they are not greatly influenced by the electric field, which heats selectively that part of the material bearing most water. Thus, the wetter inner regions get somewhat warmer. As a result of this, there is a local moisture evaporation, which causes a leveling of the moisture profile, and in general the drying rate increases due to compatible moisture and temperature gradients.

Journal Publications and Conference Presentations Arising from this Work

1) Adapa, P.K. and G.J. Schoenau, 2003. A Prototype Continuous Bed Heat Pump Dryer System for Low Temperature Drying of Specialty Crops, submitted to ASHRAE Transactions.

2) Adapa, P.K., G.J. Schoenau and S. Sokhansanj, 2002. Performance study of a heat pump dryer system for specialty crops - Part 1: Development of a Simulation Model. International Journal of Energy Research, Vol. 26: 1001-1019 (DOI: 10.1002/er.836).

3) Adapa, P.K., G.J. Schoenau and S. Sokhansanj, 2002. Performance study of a heat pump dryer system for specialty crops - Part 2: Development of a Simulation Model. International Journal of Energy Research, Vol. 26: 1021-1033 (DOI: 10.1002/er.835).

4) Adapa, P.K., G.J. Schoenau and S. Sokhansanj, 2002. Performance study of a re-circulating cabinet dryer using a household dehumidifier. International Journal of Drying Technology, Vol. 20(8): 1673-1689.

5) Adapa, P.K., G.J. Schoenau and S. Sokhansanj, 2001. An Energy Efficient System for Drying High Quality Crops in Humid Climates. The Second International Conference on Renewable Energy and Environment Protection Technologies, Cairo, Egypt, November 5 – 8.

6) Adapa, P.K., G.J. Schoenau and S. Sokhansanj, 2001. Low temperature energy efficient drying using heat pump. The 27th Annual Conference of the Solar Energy Society of Canada, Inc., Regina, Saskatchewan, September 28 – 30.

7) Adapa, P.K., S. Sokhansanj, G.J. Schoenau, and B. Crerar, 2000. Heat pump assisted drying of specialty crops. The 2000 North central region intersectional meeting sponsored by the red river valley section of the American Society of Agricultural Engineers, Moorehead, Minnesota, Paper No. RRV00-506, September 29-30.

Personnel

Person	Status
Mr. Phani Adapa (Worked initially as a graduate student on the project and later as a research engineer	Full and Part Time
Mr. Jonathan Hesseltine (Student)	Part Time
Mr. Amit Bhojkar (Graduate student)	Part Time

Information of Benefit to Producers, Processors or Government

The prototype heat pump dryer (HPD) has been turned over to Prairie Agricultural Machinery Institute (PAMI) in April 2003. It was mutually agreed that PAMI is going to resume the responsibilities of HPD day to day operations and maintenance. PAMI will also act as a central low temperature drying facility in Saskatchewan for the growers of herbs and specialty crops. The growers will have access to HPD any time and can perform necessary trials to assess their final product quality. Further, technical and experimental expertise will be provided to PAMI and growers in case they need it.